2017

Multiple Method Analysis of TiO_2 Nanoparticle Uptake in Rice (*Oryza sativa* L.) Plants

Yingqing Deng
University of Massachusetts Amherst

Elijah J. Petersen
National Institute of Standards and Technology, elijah.petersen@nist.gov

Katie E. Challis
Colorado School of Mines

Savelas A. Rabb
National Institute of Standards and Technology

R. David Holbrook
National Institute of Standards and Technology

See next page for additional authors

Authors
Yingqing Deng, Elijah J. Petersen, Katie E. Challis, Savelas A. Rabb, R. David Holbrook, James F. Ranville, Bryant C. Nelson, and Baoshan Xing

Environmental Science & Technology

Article

pubs.acs.org/est

Multiple Method Analysis of TiO_2 Nanoparticle Uptake in Rice (*Oryza sativa* L.) Plants

Yingqing Deng,[†,#] Elijah J. Petersen,[*,‡,#] Katie E. Challis,[§] Savelas A. Rabb,[∥] R. David Holbrook,[⊥] James F. Ranville,[§] Bryant C. Nelson,[‡] and Baoshan Xing[*,†]

[†]Stockbridge School of Agriculture, University of Massachusetts Amherst, 410 Paige Lab, Amherst, Massachusetts 01003, United States

[‡]Biosystems and Biomaterials Division, National Institute of Standards and Technology, 100 Bureau Drive, Building 227 Room A222, Gaithersburg, Maryland 20899, United States

[§]Department of Chemistry, Colorado School of Mines, Golden, Colorado 80401, United States

[∥]Chemical Sciences Division, National Institute of Standards and Technology, Gaithersburg, Maryland 20899, United States

[⊥]Materials Measurement Science Division, National Institute of Standards and Technology, Gaithersburg, Maryland 20899, United States

Supporting Information

ABSTRACT: Understanding the translocation of nanoparticles (NPs) into plants is challenging because qualitative and quantitative methods are still being developed and the comparability of results among different methods is unclear. In this study, uptake of titanium dioxide NPs and larger bulk particles (BPs) in rice plant (*Oryza sativa L.*) tissues was evaluated using three orthogonal techniques: electron microscopy, single-particle inductively coupled plasma mass spectroscopy (spICP-MS) with two different plant digestion approaches, and total elemental analysis using ICP optical emission spectroscopy. In agreement with electron microscopy results, total elemental analysis of plants exposed to TiO_2 NPs and BPs at 5 and 50 mg/L concentrations revealed that TiO_2 NPs penetrated into the plant root and resulted in Ti accumulation in above ground tissues at a higher level compared to BPs. spICP-MS analyses revealed that the size distributions of internalized particles differed between the NPs and BPs with the NPs showing a distribution with smaller particles. Acid digestion resulted in higher particle numbers and the detection of a broader range of particle sizes than the enzymatic digestion approach, highlighting the need for development of robust plant digestion procedures for NP analysis. Overall, there was agreement among the three techniques regarding NP and BP penetration into rice plant roots and spICP-MS showed its unique contribution to provide size distribution information.

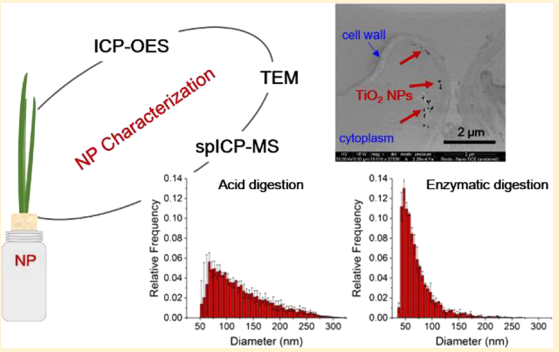

INTRODUCTION

Nanotechnology is expected to impact a wide range of industries, and the incorporation of nanomaterials into commercial products is expected to continue increasing in future years. For example, TiO_2 nanoparticles (NPs), are extensively incorporated into a large variety of commercial products, including sunscreens/cosmetics, gas sensors, pigments/coatings, construction materials (e.g., cements), food additives, drugs, and agrochemical sprays.[1,2] As a result of release from nanoenabled products, the concentration of TiO_2 NPs has been predicted to reach 16 μg/L in surface water and 0.47 mg/kg in sludge-treated soil, concentrations much higher than those predicted for ZnO NPs, Ag NPs, carbon nanotubes, or fullerenes.[3−6] In the environment, potential accumulation of TiO_2 NPs into plants may introduce these NPs into the food chain. In addition, TiO_2 NPs and SiNPs have been investigated to support the development of plants by reducing abiotic stress and decreasing uptake of cocontaminants.[7−9] Therefore, to identify and evaluate possible risks in food safety, fundamental information is needed regarding the interactions between TiO_2 NPs and plants, and robust analytical methods are needed to quantify uptake and translocation of TiO_2 NPs into plants.

Though a growing number of studies are emerging on NP interactions with terrestrial plants, available analytical techniques and associated sample pretreatment methods are limited for assessing the NPs within biological tissues. Some of the most frequently used detection techniques for NPs in plant tissues are electron microscopy (EM), X-ray absorption spectroscopy (XAS), surface enhanced Raman scattering (SERS), and total elemental analysis methods.[10−13] An early study used 2.8 nm Alizarin red S-bound (ARS) TiO_2 NPs to

Received: March 15, 2017
Revised: July 11, 2017
Accepted: August 4, 2017
Published: August 4, 2017

DOI: 10.1021/acs.est.7b01364
Environ. Sci. Technol. 2017, 51, 10615−10623

test the uptake potential in *Arabidopsis* seedlings.[14] However, the surface sites of these TiO_2 NPs were saturated with sucrose before ARS-labeling, which may have modified the NP uptake potential. In contrast with dye labeling, EM coupled with an energy dispersive X-ray spectroscopy (EDS) detector can provide direct visualization of nanomaterials and qualitative determination of their elemental compositions.[15−17] In a more recent study involving TiO_2 NPs with diameters from 14 to 655 nm, a threshold diameter of 140 nm was reported as the upper size limit for wheat uptake using a combination of techniques including scanning electron microscopy (SEM) and XAS.[15] Although this study reported that TiO_2 NPs did not undergo in vivo crystal phase modification, a mechanistic explanation describing how the TiO_2 NPs were taken up into the plants was not fully explained.[15] In addition to transmission electron microscopy (TEM)-EDS, synchrotron X-ray florescence microscopy is becoming more frequently used for in situ mapping and determination of the speciation of NPs in plant tissues.[18] However, results from both TEM and XAS analyses are usually qualitative or semiquantitative because of the substantial amount of tissue that would need to be analyzed for quantitative NP concentration results. While total elemental analysis does provide quantitative information about the total concentration of specific elements in plant tissue, this technique only detects Ti and therefore cannot distinguish between background Ti in the plant and uptake of TiO_2 NPs. Overall, the methods used to date do not provide quantitative information about uptake of TiO_2 NPs by plants, and the comparability of different measurement techniques for assessing the uptake of TiO_2 NPs into plants is unclear.

One promising analytical technique for quantifying the size distribution of NPs in biological samples is single particle inductively coupled plasma-mass spectrometry (spICP-MS). This technique has been recently used to analyze the size distribution of gold NPs and cerium dioxide NPs in plants.[19,20] However, to our knowledge, spICP-MS has not yet been used for assessing TiO_2 NPs in any organism, although spICP-MS has been used to quantify titania NPs in other environmentally relevant matrices.[21−23] The spICP-MS technique utilizes time-resolved isotopic analysis with short dwell times to characterize the particle size distribution and particle number concentration in samples.[24−27] However, the application of spICP-MS in environmentally/biologically relevant samples is still largely limited by uncertainty in the robustness of different extraction methods and interferences from natural matrices.

In the present study, uptake of TiO_2 NPs in hydroponically grown rice plants was comprehensively evaluated using three orthogonal techniques. After the exposure period, plants were evaluated using EM and bulk elemental analysis of acid extracts via inductively coupled plasma-optical emission spectroscopy (ICP-OES). A newly developed spICP-MS method was also applied to the extracts obtained with two different extraction methods (enzymatic and acidic). The comparability of the results from the different methods was evaluated.

MATERIALS AND METHODS

Characterization of TiO_2 Particles. TiO_2 NPs (SRM 1898, 99.5% purity) were acquired from the National Institute of Standards and Technology (NIST; Gaithersburg, MD) with primary particle sizes from 19 to 37 nm and a mixed-phase crystal structure consisting of anatase and rutile polymorphs. The specific surface area of SRM 1898 has been previously characterized as (55.55 ± 0.70) m^2/g.[28,29] Elementally similar TiO_2 bulk particles (BPs, purity 98.0% to 100.5%) were purchased from Acros Organics (New Jersey, USA). The hydrodynamic size and zeta potential of TiO_2 NPs were measured in deionized water using dynamic light scattering (DLS, Zetasizer Nano, Malvern) shortly prior to exposure. The intensity-based hydrodynamic diameters were measured using 173° backscatter detection at 25 °C; at least three replicates were tested per condition and each run had at least 3 subruns. For all plant experiments, the TiO_2 NP and BP suspensions were prepared in Milli-Q water at 5 mg/L and 50 mg/L and dispersed with a probe sonicator (Misonix S-4000, Farmingdale, NY) at a delivered power of 50 W and in 80% pulsed mode for 15 min.[28,30,31] Samples from the suspensions were then transferred into disposable 3 mL polystyrene cuvettes and shipped to NIST for measurement of the total Ti concentration. A minimum of three individual samples were tested from each suspension. spICP-MS analysis was also conducted on separately prepared samples. For the TEM specimen preparation, ∼5 μL of the TiO_2 suspension was pipetted onto TEM grids (200 mesh, Ted Pella, Redding, CA) and allowed to dry. The samples were then characterized using a JEOL 2000FX TEM operating at an accelerating voltage of 200 kV. Characterizations results including TEM, DLS, and ICP-OES analyses of the suspended NPs and BPs are provided in the Supporting Information (SI) and in Figure S1 and Tables S1 and S2. While the DLS size measurements showed an average agglomerate size of greater than 100 nm for the TiO_2 NPs, TEM and spICP-MS analyses indicated that the majority of the particles were typically less than 100 nm.

Plant Cultivation and Exposure Assay. Rice seeds (*Oryza sativa* L., Nipponbare) were obtained from the USDA Dale Bumpers National Rice Research Center (Stuttgart, Arkansas). Following surface sterilization in a 5% bleach solution for 15 min and heat stimulation in a 50 °C water bath for 4 h, seeds were allowed to germinate on moist filter papers in sterile Petri dishes until the development of the first true leaf. Selected uniform rice seedlings were then transplanted into aerated hydroponic pots in a greenhouse (University of Massachusetts, Amherst). Rice plants grew under the controlled average temperature of 24 and 18 °C during the day and night, respectively, with 4 h supplemental light after sunset (PAR source, 5.8 $mol \cdot m^{-2} \cdot d^{-1}$). Each pot was used to expose five rice plants after filling with 3.6 L Hoagland nutrient solution. The Hoagland media contained macronutrients (288 mg/L $NaNO_3$, 38 mg/L NaH_2PO_4, 446 mg/L KCl, 555 mg/L $CaCl_2$, and 240 mg/L $MgSO_4$) and micronutrients (0.5 mg/L H_3BO_3, 0.5 mg/L $MnCl_2 \cdot 4H_2O$, 0.05 mg/L $ZnSO_4 \cdot 7H_2O$, 0.02 mg/L $CuSO_4 \cdot 5H_2O$, 0.01 mg/L $H_2MoO_4 \cdot H_2O$, and 1.0 mg/L NaFe-EDDHA).

After assimilation for 3 d in Hoagland solution, the rice plants were exposed to nominal concentrations of 0, 5, and 50 mg/L TiO_2 NPs (prepared in Milli-Q water) for 24 h in separate glass containers wrapped with aluminum foil, while 5 and 50 mg/L TiO_2 BPs were used for comparison. Each treatment had 7 identical containers as replicates, and each container had 5 plants. After exposure for 24 h, some plants from each container were used for DNA damage[29,32,33] and antioxidant enzyme activity analyses. A description of the methods and results are described in the SI. The remaining plants were carefully rinsed and transferred to Hoagland nutrient solution without TiO_2 and were then incubated for another 3 d after which point they were used for EM, total Ti, spICP-MS, and antioxidant enzyme activity analyses. Upon

DOI: 10.1021/acs.est.7b01364
Environ. Sci. Technol. 2017, 51, 10615−10623

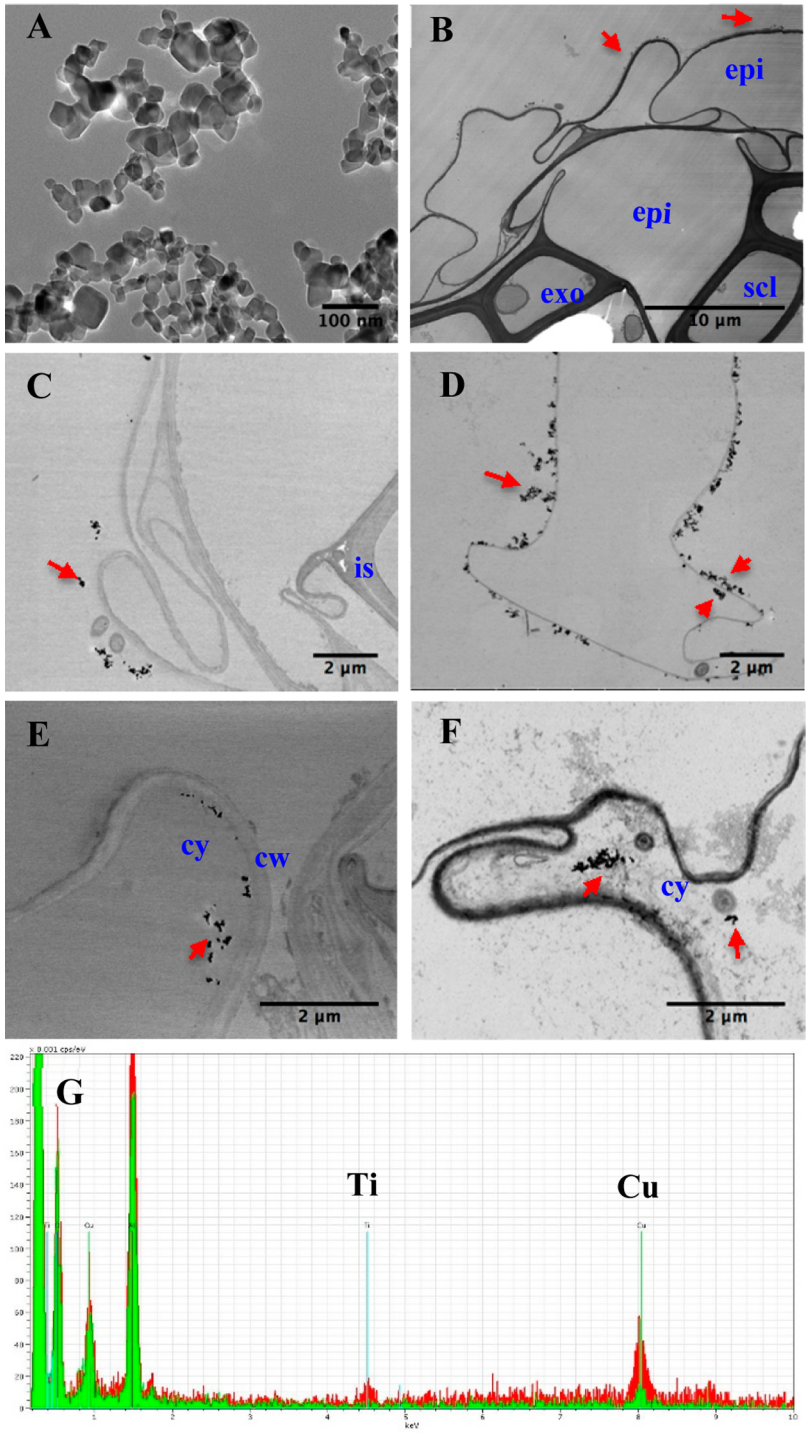

Figure 1. Transmission electron micrographs of TiO_2 NPs under 20 kV. (A) TiO_2 NPs were characterized after dispersion in Milli-Q water; (B–F) Transverse root sections of rice (*Oryza sativa* L.) grown in 50 mg/L TiO_2 NP suspension for 24 h were observed under STEM-EDS. Microstructure, as denoted in blue, included exodermis (exo), sclerenchyma (scl), epidermis (epi), cell wall (cw), intercellular space (is), and cytoplasm (cy). Condensed dark spots, shown with red arrow, represented TiO_2 NPs and were identified as Ti through energy-dispersive spectroscopy. In the EDS figure (G), the red spectrum is an example of an area with Ti-containing particles while the green spectrum is a background spectrum that does not contain nanoparticles. Copper signals come from the grids.

harvest, the plants were rinsed with running distilled water for at least 5 min, dried with paper towels using intermittent blotting, and then rinsed with running deionized water. For total Ti analysis, rice plants were separated into roots and leaves, digested with nitric and hydrofluoric acid, and analyzed using ICP-OES as described in the SI. For spICP-MS analysis, the roots and shoots were combined from several plants. The plant samples were treated with enzymatic (Macerozyme R-10) or acidic (12 mL of a 3:1 by volume mixture of concentrated nitric and hydrochloric acid) microwave digestion approaches prior to spICP-MS analysis; full details for the digestion approaches and spICP-MS analysis are provided in the SI. The actual concentration that the plants were exposed to and the settling of the NPs or BPs in the absence or presence of plants

DOI: 10.1021/acs.est.7b01364
Environ. Sci. Technol. 2017, 51, 10615–10623

for 24 h was analyzed using ICP-OES as described in the SI. Samples were taken immediately after sonication for the initial samples, while 20 mL samples were taken later after 24 h of settling in containers with or without plants to assess changes in the TiO_2 particle concentration during the exposure interval.

Analysis of TiO_2 Nanoparticle Uptake Using Scanning Transmission Electron Microscopy (STEM). Roots and shoots were sampled for direct observation of TiO_2 NPs in vivo. Tissues were prefixed in monobasic phosphate buffer containing 4% formaldehyde and 1% glutaraldehyde (pH 7.2 to pH 7.4) for 2 h under vacuum, and postfixed in 1% osmium tetroxide/0.1 mol/L phosphate buffer for 1 h at room temperature. Subsequently, tissues were rinsed with a graded ethanol series (50% to 100% ethanol) and then with acetone. Following infiltration and embedding with Spurr's low viscosity resin,[33,34] the epoxy resin was polymerized in a 60 °C oven for 24 h. Blocks containing plant tissues were sectioned on an ultracut microtome (Ultracut E, Reicher-Jung) to provide 60 nm to 90 nm thin sections and loaded onto 200 mesh uncoated copper grids. Sample stubs were placed in an environmental scanning electron microscope (Quanta 200F, FEI, Hillsboro, OR), operating at high vacuum, for both imaging and compositional analysis via X-ray EDS (EDAX, Inc.).

Statistical Analysis. All analyses were conducted using GraphPad Prism (version 5). ICP-OES, DNA damage, and oxidative biomarker data were tested for outliers using the Grubb's test. For conditions with $n = 3$, the data also had to deviate more than 50% from the next closest value before being removed as an outlier. Significant differences among conditions were statistically analyzed using one-way ANOVA followed by Tukey's multiple comparison test for comparison among all sample sets or Dunnett's multiple comparison test for comparisons only against the control treatment; all samples analyzed statistically had at least three data points. Statistical significance (when not specified) was based on a probability of $p < 0.05$.

RESULTS AND DISCUSSION

STEM Imaging of TiO_2 NPs. The roots and leaves from plants treated with 50 mg/L TiO_2 NPs were sampled and analyzed with STEM-EDS. There were no noticeable morphology changes in rice plants. STEM analysis showed that TiO_2 NPs extensively covered the root epidermal surface (Figure 1B–D). The accumulation on the epidermal surface may be through mechanical adhesion or diffusion, a finding previously observed with ZnO NPs and CeO_2 NPs or CuO NPs on the roots of corn or wheat plants, respectively.[35−39] Within the cytoplasm of the treated roots, electron dense dark deposits were recognized occasionally and confirmed to be elemental Ti through EDS analysis (Figure 1). These Ti-rich deposits were not observed in control plants (not shown). While the distribution of intracellular TiO_2 NPs followed no clear pattern, particles were more frequently found in root outer layers and tended to appear as agglomerates near plasma membranes (Figure 1D and E). In wheat (*Triticum aestivum spp.*), it was also observed that TiO_2 NPs (exposure at 100 mg/L) were entrapped in endosome or vacuole-like structures.[15] Unlike what was reported for wheat, TiO_2 NP clusters in rice roots did not show affinity for certain cell organelles, but appeared as free NPs close to plasma membranes. In a study on the uptake of TiO_2 using cucumber (*Cucumis sativus*), TiO_2 particles were found using micro X-ray fluorescence and micro X-ray absorption spectroscopy to penetrate into the transport system.[18,40] In agreement with those results obtained from exposed cucumber and wheat, TiO_2 NPs were able to penetrate rice roots and enter into root cells as confirmed through STEM-EDS, which is the first direct evidence of TiO_2 NPs uptake in rice plant root cells. This solid evidence of TiO_2 internalization by plant cells was also consistent with results for a variety of other metal-based nanoparticles, including Fe_3O_4, Au, and Cu nanoparticles.[41−45] Intracellular TiO_2 NP clusters may result from the agglomeration of internalized individual particulates under the dynamic physiological environment in the cytoplasm.

After internalization, TiO_2 NPs have the potential to translocate into the shoots and even into edible regions. However, no obvious accumulation of TiO_2 clusters was observed in rice leaf tissues through STEM observation, probably because of limited transfer from roots to shoot and the lower exposure concentration relative to other studies.[15,18] Larue et al. reported 36 nm as the upper threshold diameter for TiO_2 NPs to translocate from root to leaves in wheat, while Servin et al. used micro-X-ray absorption near edge spectroscopy spectra to reveal the presence of TiO_2 NPs (Degussa P25) in cucumber leaf tissues suggesting that larger agglomerates similar to those prepared in this study can also be internalized by some plants.[15,18] TiO_2 NPs have negligible ion release at the pH used in this study and are reported to remain in the same chemical form in vivo,[18,46,47] a result confirmed in this study through elemental analysis after filtering particle suspensions that had been acid treated and not finding detectable dissolved Ti (see SI). Thus, it is improbable that Ti ions were absorbed into the plants and then reformed into particles.

Trends in Titanium Accumulation in Plant Tissues. With the evidence of observable TiO_2 NPs in rice plants, ICP-OES was further employed to quantify the element accumulation over time in the roots and shoots (Figure 2).

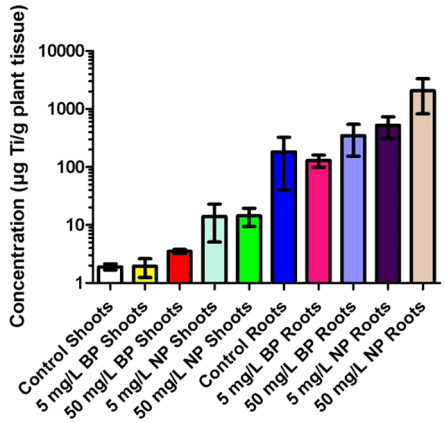

Figure 2. Titanium accumulation in rice roots and shoots resulting from TiO_2 NP and BP exposure. Each data point represents the mean ± SD, for 2 or 3 samples (plantlets were combined into 3 replicates but some results were removed as a result of being outliers). Note the logarithmic scale for the *y*-axis.

Titanium accumulated in the shoots at a considerably lower level than in the roots, with a roughly 2 orders of magnitude difference. Despite vigorously washing the roots, this difference may partly stem from the titanium root concentration including particles adhering to the external surfaces of the roots in addition to particles inside the roots, while the concentration measured in the stems only included internalized titanium.

DOI: 10.1021/acs.est.7b01364
Environ. Sci. Technol. 2017, 51, 10615−10623

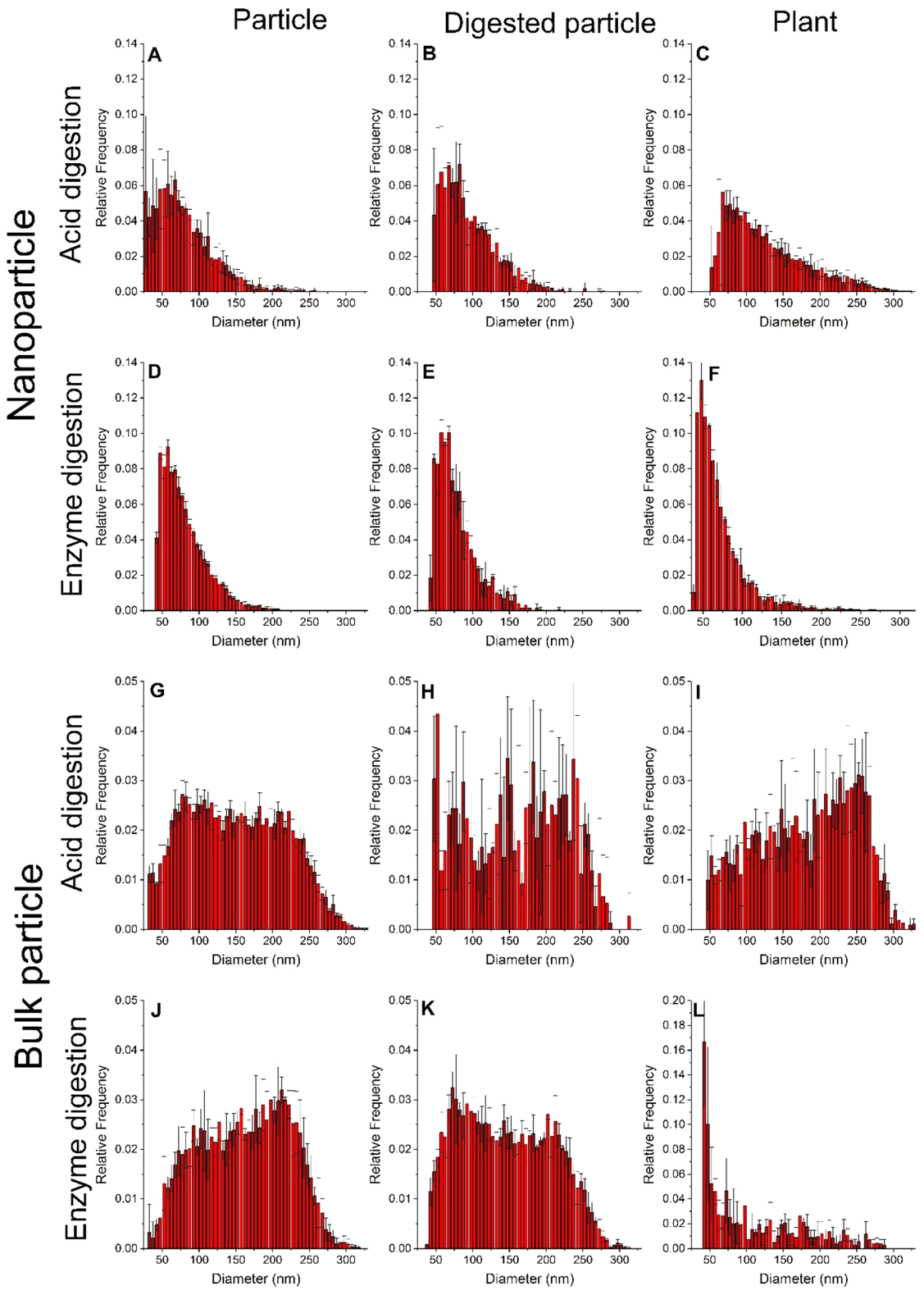

Figure 3. spICP-MS analysis of the acid digestion and 24 h enzyme digestion treatments for the samples. Size distributions are normalized to relative frequency. All graphs are the averages of triplicate samples and error bars represent standard deviation values. Particles dispersed in water without treatment for NPs (A and D) and BPs (G and J). The results shown in part A and G versus D and J were from samples analyzed on the same day as the samples which were treated with the acid digestion and enzyme extraction, respectively. Differences between the results reflect the day-to-day variability in spICP-MS analysis of TiO_2 NPs. NPs which were acid digested (B) or digested using enzymes for 24 h (E). BPs that were acid digested (H) or digested using enzymes for 24 h (K). Microwave acid digested plants, which were exposed to NPs (C) or BPs (I). Plants exposed to NPs (F) or BPs (L), following 24 h of enzyme digestion. The samples in parts A–C and G–I were analyzed the same day as the samples in parts D–F and J–L. Changes in the size detection limit were not from dissolved Ti in either digestion.

DOI: 10.1021/acs.est.7b01364
Environ. Sci. Technol. 2017, 51, 10615–10623

Characterization of TiO_2 NP and BP Uptake Using spICP-MS. In addition to characterizing the total Ti in the plant tissues, it is important to assess the size distribution and number concentration of the particles in the tissues. This was accomplished via spICP-MS analysis using two different extraction methods: microwave acid digestion and an enzymatic digestion that was previously used to extract gold NPs from tomato plants.[19]

According to multiple control measurements, neither the enzymatic nor acid digestion procedures clearly changed the size distribution of the NPs or BPs (Figures 3 and S2 and Tables 1 and 2). For the NP treatment, an increase in the value for the smallest bin size above the background was observed for the acid-treated control samples (Figure 3B compared to 3A; 32 nm increased to 47 nm) but not the enzyme-treated samples (Figure 3E compared to 3D). The size detection limit was determined by background counts in the control medias, but some of the detection limit variation may be due to slight daily changes in instrument performance. Importantly, the size detection limit was not impacted by dissolved Ti; measurements of the dissolved Ti concentration determined by ICP-OES analysis of the NPs following the acid digestion treatment and filtration with a 0.02 μm pore size filter were never greater than the instrument detection limit (0.0006 mg/L Ti). Reagent control samples (without particles) did show a small number of pulses that were interpreted as particles, but most of these pulses were just above the background cutoff and therefore were interpreted as NPs just above the size detection limit (Figures S3–S5). The presence of a small number of large pulses in the control matrix is not surprising given that analysis of water or 2% nitric acid blank yields a small number of peaks (5 to 50) during a 60 s analysis for Ti. The peaks observed in blanks are thought to be dust or particles that were located in the sample introduction system and became dislodged during sample analysis (Figures S4 and S5). In this experiment, the acid matrix showed an average of 42 ± 11 peaks during a 60 s run and the 24 h enzyme matrix was slightly higher with an average of 77 ± 20 peaks; Figure S4 shows a comparison between the acid matrix and the number of spikes for a NP exposed plant treated with the acid digestion approach. It is also important to note the total Ti in controls (spICP-MS data shown in Figures S3 and S4) is below or at the limit of detection when doing total elemental analysis of Ti. Treatment of control plant samples (not exposed to particles) resulted in spikes that could be interpreted as particles, with an average of 390 ± 190 peaks in the enzyme digestion samples and 150 ± 112 peaks in the acid digestion samples. In comparison, the number of peaks detected in NP exposed plant samples was 5080 ± 1970 and 2390 ± 1850 pulses for the acid digestion and 24 h enzyme digestion, respectively. Figure 4 shows the size distribution of these apparent particles in the control plants. Although there were more peaks in the enzyme digested control plants, the particles are calculated to be near the size detection limit, probably outliers in background signal that were not removed during data processing (Figure 4). The pulses in the acid treatment of the control plants were larger. The instrumental transport efficiency and dilution factors were used to calculate how many particles were detected per plant for control, NP-exposed, and BP-exposed plants by each digestion method (Table S3). In the acid treatment, there are approximately 50× more particles in the NP-exposed plants and 5× more particles in the BP-exposed plants than in the control plants.

For the NP-exposed plants treated with the acid digestion process, there was an increase in the breadth of the distribution (Figure 3C and S6C) as indicated by a greater number of particles in the tail to the right of the main distribution. This result contrasts with the data from the enzymatic digested NP-exposed plants, which show distributions more similar to those of the NP control (without NP or BP exposure) (Figures 3 and S3). While there is an increase in frequency for the 24 and 48 h enzymatic treatments in the range of 45 to 60 nm for these samples as compared to the NP control treatments, this result could be impacted by the background subtraction process. The broader size distribution of the NP-exposed plants after treatment with the acid digestion process could stem from changes to the NPs caused by the acid treatment or as a result of the enzymatic process being a less efficient extraction process of the plant tissues and not liberating larger particles that were associated with the plant tissue; however, control experiments did not show a change in the size distribution to the NPs after the acid treatment (Figure 3). It was clear from visual inspection that a larger fraction of undigested plant material remained after the enzymatic process and the average total amount of Ti extracted from the plants was approximately 6×

Table 1. spICP-MS Analysis of the Enzyme Digestion Samples (n = 3)

sample	mean diameter ± standard deviation (nm)	mode diameter (nm)
NP in Milli-Q (no treatment)	79 ± 30	48
BP in Milli-Q (no treatment)	161 ± 60	206
24 h enzyme digestion treated samples		
enzyme only control (no added particles)	81 ± 49	43
control plants	58 ± 30	42
NP in enzyme	78 ± 28	56
plants exposed to NPs	71 ± 31	44
BP in enzyme	145 ± 62	74
plants exposed to BPs	107 ± 66	42
48 h enzyme digestion treated samples		
enzyme only control (no added particles)	70 ± 30	50
control plant	68 ± 35	48
NP in enzyme	76 ± 29	48
plants exposed to NPs	70 ± 30	42
BP in enzyme	136 ± 56	84
plants exposed to BPs	116 ± 63	60

Table 2. spICP-MS Analysis of the Acid-Digestion Samples (n = 3)

sample	mean diameter ± standard deviation (nm)	mode diameter (nm)
NP in Milli-Q (no treatment)	78 ± 38	34
BP In Milli-Q (no treatment)	150 ± 65	95
acid digestion treated samples		
acid control (no added particles)	112 ± 65	58
control plants	124 ± 57	60
NP in acid	94 ± 36	52
plants exposed to NPs	126 ± 53	65
BP in acid	159 ± 67	128
plants exposed to BPs	181 ± 67	236

DOI: 10.1021/acs.est.7b01364
Environ. Sci. Technol. 2017, 51, 10615–10623

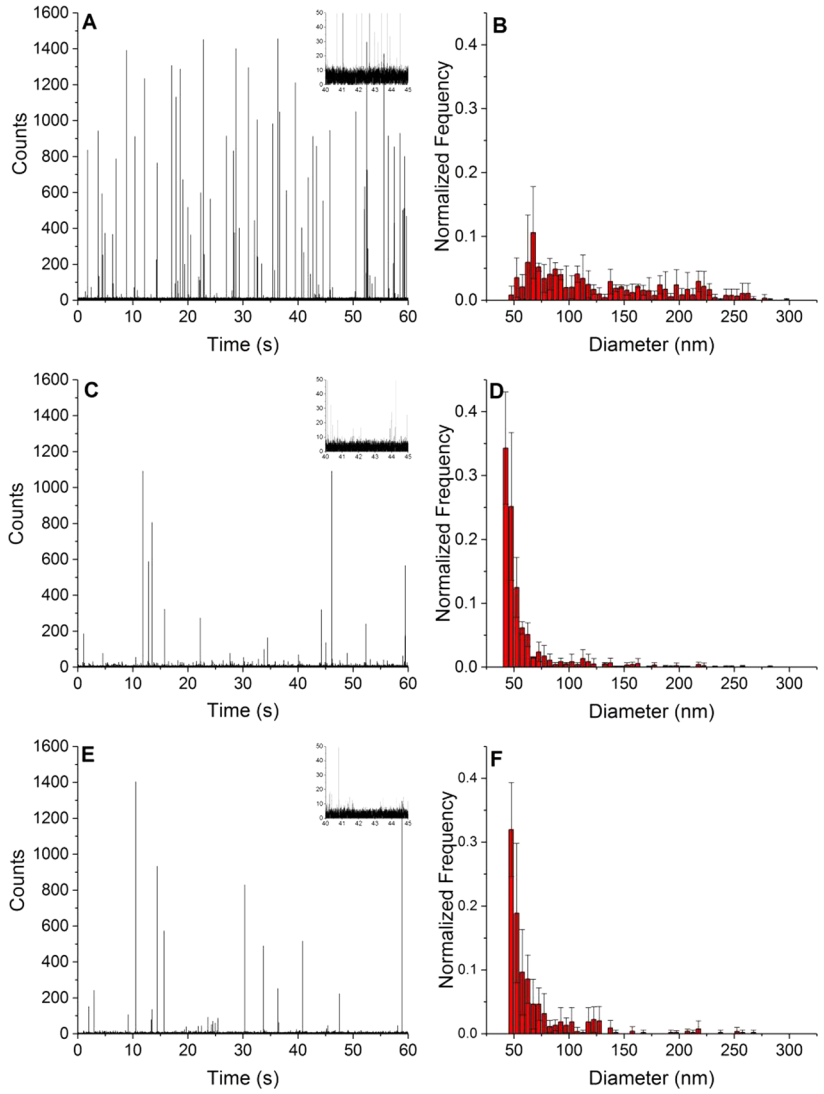

Figure 4. Example graphs of raw single particle data, pulses are interpreted as particles, for digestion of control plants using acid (A), 24 h enzymatic (C), or 48 h enzymatic (E) treatments. Insets zoom in on five seconds of data to reveal the background. Relative frequency for digestion of control plants using acid (B), 24 h enzymatic (D), or 48 h enzymatic (F) treatments; graphs are the averages of triplicate samples and error bars represent standard deviation values.

higher for the acid digestion compared to the enzymatic digestion as determined by integrating and summing the spICP-MS peaks.

The plants exposed to the BP treatment showed a similar size distribution for the acid digestion procedure to BP controls in ultrapure water, while a substantially higher frequency of smaller particles was observed for the 24 and 48 h enzyme extraction procedure (Figures 3, S3, and S6), a result similar to that observed for the NP-exposed plants. The increase in the number of smaller particles for the enzymatic extraction procedures may be partially due to the background cutoff procedure not removing some background counts or from the enzyme process being less efficient than the acid digestion procedure with regards to extracting larger particles. The macerozyme is a mixture of cellulase, hemicellulase, and pectinase, and is designed to break down the cell walls of plant cells. Since there was still plant matter clearly visible in the digestion following 48 h, it is possible that not all cell walls were destroyed and perhaps remained sufficiently intact to retain the larger BPs.

Overall, both acid and enzyme digestion methods successfully extracted particles from the plant tissues, and there was a clear difference in size distribution of extracted TiO_2 particles for the plants exposed to the BPs and NPs. The size distribution for the NP exposed plants had a narrower size distribution which contained predominately smaller particles while the BP exposed plants showed a much broader distribution with a larger fraction of particles with sizes greater than 100 nm. This indicates that spICP-MS was able to identify a difference in the particle size distribution among the NP and BP treatments, which is a finding that could not be readily obtained using total elemental analysis or electron microscopy. However, the precision of this result was impacted by limitations regarding the efficiency of the enzymatic digestion procedures for particles with larger sizes and uncertainty from the background subtraction step for particles smaller than ~55 nm. The value of EM analysis is that it provided definitive identification of the NPs in the plant tissues and also information about the distribution of the NPs within the tissues but only a small fraction of the plant area can be

DOI: 10.1021/acs.est.7b01364
Environ. Sci. Technol. 2017, 51, 10615−10623

analyzed within a reasonable time period. Total elemental analysis also provided complementary information to spICP-MS given that the recovery of the Ti from the digestion procedure could be readily quantified such as by comparing the concentration measured using ICP-OES to the concentration from an orthogonal Ti quantification methods (e.g., neutron activation analysis). However, orthogonal methods are not yet available for comparison of the size distribution of NPs measured after spICP-MS extractions, but the total quantity of Ti measured after different extraction procedures and spICP-MS analyses could be compared to that for the total elemental analysis. Overall, each technique provided important, complementary insights into the bioaccumulation behaviors of NPs and BPs within the rice plant.

■ ASSOCIATED CONTENT

Supporting Information

The Supporting Information is available free of charge on the ACS Publications website at DOI: 10.1021/acs.est.7b01364.

ICP-OES analysis of plant samples and settling of TiO_2 NPs and BPs, spICP-MS analysis of the plant samples, determination of CAT, POD, APX, and SOD activities, DNA damage measurements, characterization of TiO_2 particles, antioxidant enzymes and oxidatively induced DNA base damage, initial concentrations of NPs and BPs after settling for 24 h in the presence and absence of plants, hydrodynamic diameter (size) of TiO_2 nanoparticles in Milli-Q water before and after plant exposure, average number of nanoparticles detected per gram of plant tissue for control, NP-exposed, and BP-exposed plants, TEM images of TiO_2 NPs and BPs, spICP-MS analysis of 48 h enzymatic digestion data for NPs and BPs, spICP-MS analysis reagent control samples (without particles) treated with the different digestion procedures, example of spICPMS signals detected in acid matrix and an acid-digested NP-exposed plant, raw data for MilliQ water and relative frequency from three samples of MilliQ, mass weighted size distribution summary of spICP-MS results for the acid digestion procedure samples, content of superoxide dismutase (SOD), ascorbate peroxidase (APX), catalase (CAT), and peroxidase (APX) in *Oryza sativa* whole plant extracts, and oxidatively induced DNA base lesions (PDF)

■ AUTHOR INFORMATION

Corresponding Authors

*E-mail: elijah.petersen@nist.gov. Tel: 301-975-8142.
*E-mail: bx@umass.edu. Tel: 413-545-5212.

ORCID

Elijah J. Petersen: 0000-0001-8215-9127
Baoshan Xing: 0000-0003-2028-1295

Author Contributions

#Y.D. and E.J.P. contributed equally to this work.

Notes

The authors declare no competing financial interest.

■ ACKNOWLEDGMENTS

This research was supported by USDA NIFA Hatch Program (MAS 00475) and EPA grant RD83558001. Mention of trade names or commercial products is solely for the purpose of providing specific information and does not imply recommendation or endorsement by the National Institute of Standards and Technology. We thank Vincent Hackley and Julian Taurozzi (NIST) for providing samples of SRM 1898 and for assistance with the dispersion protocol.

■ REFERENCES

(1) Weir, A.; Westerhoff, P.; Fabricius, L.; Hristovski, K.; von Goetz, N. Titanium Dioxide Nanoparticles in Food and Personal Care Products. *Environ. Sci. Technol.* **2012**, *46* (4), 2242−2250.

(2) Chen, X.; Mao, S. S. Titanium Dioxide Nanomaterials: Synthesis, Properties, Modifications, and Applications. *Chem. Rev.* **2007**, *107* (7), 2891−2959.

(3) Gottschalk, F.; Sonderer, T.; Scholz, R. W.; Nowack, B. Modeled Environmental Concentrations of Engineered Nanomaterials (TiO2, ZnO, Ag, CNT, Fullerenes) for Different Regions. *Environ. Sci. Technol.* **2009**, *43* (24), 9216−9222.

(4) Gottschalk, F.; Sun, T. Y.; Nowack, B. Environmental concentrations of engineered nanomaterials: Review of modeling and analytical studies. *Environ. Pollut.* **2013**, *181*, 287−300.

(5) Mueller, N. C.; Nowack, B. Exposure modeling of engineered nanoparticles in the environment. *Environ. Sci. Technol.* **2008**, *42* (12), 4447−4453.

(6) Musee, N. Simulated environmental risk estimation of engineered nanomaterials: A case of cosmetics in Johannesburg City. *Hum. Exp. Toxicol.* **2011**, *30* (9), 1181−1195.

(7) Cai, F.; Wu, X.; Zhang, H.; Shen, X.; Zhang, M.; Chen, W.; Gao, Q.; White, J. C.; Tao, S.; Wang, X. Impact of TiO 2 nanoparticles on lead uptake and bioaccumulation in rice (Oryza sativa L.). *NanoImpact* **2017**, *5*, 101−108.

(8) Tripathi, D. K.; Singh, S.; Singh, V. P.; Prasad, S. M.; Chauhan, D. K.; Dubey, N. K. Silicon Nanoparticles More Efficiently Alleviate Arsenate Toxicity than Silicon in Maize Cultiver and Hybrid Differing in Arsenate Tolerance. *Front. Environ. Sci.* **2016**, *4*, 46.

(9) Liu, H.; Ma, C.; Chen, G.; White, J. C.; Wang, Z.; Xing, B.; Dhankher, O. P. Titanium Dioxide Nanoparticles Alleviate Tetracycline Toxicity to Arabidopsis thaliana (L.). *ACS Sustainable Chem. Eng.* **2017**, *5* (4), 3204−3213.

(10) Bandyopadhyay, S.; Peralta-Videa, J. R.; Gardea-Torresdey, J. L. Advanced Analytical Techniques for the Measurement of Nanomaterials in Food and Agricultural Samples: A Review. *Environ. Eng. Sci.* **2013**, *30* (3), 118−125.

(11) Zhang, Z.; Guo, H.; Deng, Y.; Xing, B.; He, L. Mapping gold nanoparticles on and in edible leaves in situ using surface enhanced Raman spectroscopy. *RSC Adv.* **2016**, *6* (65), 60152−60159.

(12) Hassellov, M.; Readman, J. W.; Ranville, J. F.; Tiede, K. Nanoparticle analysis and characterization methodologies in environmental risk assessment of engineered nanoparticles. *Ecotoxicology* **2008**, *17* (5), 344−361.

(13) Handy, R. D.; van den Brink, N.; Chappell, M.; Muehling, M.; Behra, R.; Dusinska, M.; Simpson, P.; Ahtiainen, J.; Jha, A. N.; Seiter, J.; Bednar, A.; Kennedy, A.; Fernandes, T. F.; Riediker, M. Practical considerations for conducting ecotoxicity test methods with manufactured nanomaterials: what have we learnt so far? *Ecotoxicology* **2012**, *21* (4), 933−972.

(14) Kurepa, J.; Paunesku, T.; Vogt, S.; Arora, H.; Rabatic, B. M.; Lu, J. J.; Wanzer, M. B.; Woloschak, G. E.; Smalle, J. A. Uptake and Distribution of Ultrasmall Anatase TiO2 Alizarin Red S Nanoconjugates in Arabidopsis thaliana. *Nano Lett.* **2010**, *10* (7), 2296−2302.

(15) Larue, C.; Laurette, J.; Herlin-Boime, N.; Khodja, H.; Fayard, B.; Flank, A. M.; Brisset, F.; Carriere, M. Accumulation, translocation and impact of TiO2 nanoparticles in wheat (Triticum aestivum spp.): Influence of diameter and crystal phase. *Sci. Total Environ.* **2012**, *431*, 197−208.

(16) Larue, C.; Pinault, M.; Czarny, B.; Georgin, D.; Jaillard, D.; Bendiab, N.; Mayne-L'Hermite, M.; Taran, F.; Dive, V.; Carriere, M.

DOI: 10.1021/acs.est.7b01364
Environ. Sci. Technol. 2017, 51, 10615−10623

Quantitative evaluation of multi-walled carbon nanotube uptake in wheat and rapeseed. *J. Hazard. Mater.* **2012**, *227-228*, 155−163.
(17) Fan, R. M.; Huang, Y. C.; Grusak, M. A.; Huang, C. P.; Sherrier, D. J. Effects of nano-TiO2 on the agronomically-relevant Rhizobium-legume symbiosis. *Sci. Total Environ.* **2014**, *466-467*, 503−512.
(18) Servin, A. D.; Castillo-Michel, H.; Hernandez-Viezcas, J. A.; Diaz, B. C.; Peralta-Videa, J. R.; Gardea-Torresdey, J. L. Synchrotron Micro-XRF and Micro-XANES Confirmation of the Uptake and Translocation of TiO2 Nanoparticles in Cucumber (Cucumis sativus) Plants. *Environ. Sci. Technol.* **2012**, *46* (14), 7637−7643.
(19) Dan, Y.; Zhang, W.; Xue, R.; Ma, X.; Stephan, C.; Shi, H. Characterization of Gold Nanoparticle Uptake by Tomato Plants Using Enzymatic Extraction Followed by Single-Particle Inductively Coupled Plasma−Mass Spectrometry Analysis. *Environ. Sci. Technol.* **2015**, *49* (5), 3007−3014.
(20) Dan, Y.; Ma, X.; Zhang, W.; Liu, K.; Stephan, C.; Shi, H. Single particle ICP-MS method development for the determination of plant uptake and accumulation of CeO2 nanoparticles. *Anal. Bioanal. Chem.* **2016**, *408* (19), 5157−5167.
(21) Donovan, A. R.; Adams, C. D.; Ma, Y.; Stephan, C.; Eichholz, T.; Shi, H. Single particle ICP-MS characterization of titanium dioxide, silver, and gold nanoparticles during drinking water treatment. *Chemosphere* **2016**, *144*, 148−153.
(22) Vidmar, J.; Milačič, R.; Ščančar, J. Sizing and simultaneous quantification of nanoscale titanium dioxide and a dissolved titanium form by single particle inductively coupled plasma mass spectrometry. *Microchem. J.* **2017**, *132*, 391−400.
(23) Dan, Y.; Shi, H.; Stephan, C.; Liang, X. Rapid analysis of titanium dioxide nanoparticles in sunscreens using single particle inductively coupled plasma−mass spectrometry. *Microchem. J.* **2015**, *122*, 119−126.
(24) Pace, H. E.; Rogers, N. J.; Jarolimek, C.; Coleman, V. A.; Higgins, C. P.; Ranville, J. F. Determining Transport Efficiency for the Purpose of Counting and Sizing Nanoparticles via Single Particle Inductively Coupled Plasma Mass Spectrometry. *Anal. Chem.* **2011**, *83* (24), 9361−9369.
(25) Montano, M. D.; Badiei, H. R.; Bazargan, S.; Ranville, J. F. Improvements in the detection and characterization of engineered nanoparticles using spICP-MS with microsecond dwell times. *Environ. Sci.: Nano* **2014**, *1* (4), 338−346.
(26) Montoro Bustos, A. R.; Petersen, E. J.; Possolo, A.; Winchester, M. R. Post hoc Interlaboratory Comparison of Single Particle ICP-MS Size Measurements of NIST Gold Nanoparticle Reference Materials. *Anal. Chem.* **2015**, *87* (17), 8809−8817.
(27) El Hadri, H.; Petersen, E. J.; Winchester, M. R. Impact of and correction for instrument sensitivity drift on nanoparticle size measurements by single-particle ICP-MS. *Anal. Bioanal. Chem.* **2016**, *408* (19), 5099−5108.
(28) Taurozzi, J. S.; Hackley, V. A.; Wiesner, M. R. A standardised approach for the dispersion of titanium dioxide nanoparticles in biological media. *Nanotoxicology* **2013**, *7* (4), 389−401.
(29) Petersen, E. J.; Reipa, V.; Watson, S. S.; Stanley, D. L.; Rabb, S. A.; Nelson, B. C. DNA Damaging Potential of Photoactivated P25 Titanium Dioxide Nanoparticles. *Chem. Res. Toxicol.* **2014**, *27* (10), 1877−1884.
(30) Taurozzi, J. S.; Hackley, V. A.; Wiesner, M. R. Ultrasonic dispersion of nanoparticles for environmental, health and safety assessment - issues and recommendations. *Nanotoxicology* **2011**, *5* (4), 711−729.
(31) Taurozzi, J. S.; Hackley, V. A.; Wiesner, M. R. *Preparation of Nanoscale TiO2 Dispersions in Biological Test Media for Toxicological Assessment*, NIST Special Publication 1200-4; National Institute of Standards and Technology: Gaithersburg, MD, 2012. DOI: 10.6028/NIST.SP.1200-4.
(32) Petersen, E. J.; Nelson, B. C. Mechanisms and measurements of nanomaterial-induced oxidative damage to DNA. *Anal. Bioanal. Chem.* **2010**, *398* (2), 613−650.
(33) Atha, D. H.; Wang, H. H.; Petersen, E. J.; Cleveland, D.; Holbrook, R. D.; Jaruga, P.; Dizdaroglu, M.; Xing, B. S.; Nelson, B. C. Copper Oxide Nanoparticle Mediated DNA Damage in Terrestrial Plant Models. *Environ. Sci. Technol.* **2012**, *46* (3), 1819−1827.
(34) Spurr, A. R. A low-viscosity epoxy resin embedding medium for electron microscopy. *J. Ultrastruct. Res.* **1969**, *26* (1−2), 31−43.
(35) Lin, D.; Xing, B. Root uptake and phytotoxicity of ZnO nanoparticles. *Environ. Sci. Technol.* **2008**, *42* (15), 5580−5585.
(36) Wild, E.; Jones, K. C. Novel Method for the Direct Visualization of in Vivo Nanomaterials and Chemical Interactions in Plants. *Environ. Sci. Technol.* **2009**, *43* (14), 5290−5294.
(37) Zhao, L. J.; Peralta-Videa, J. R.; Ren, M. H.; Varela-Ramirez, A.; Li, C. Q.; Hernandez-Viezcas, J. A.; Aguilera, R. J.; Gardea-Torresdey, J. L. Transport of Zn in a sandy loam soil treated with ZnO NPs and uptake by corn plants: Electron microprobe and confocal microscopy studies. *Chem. Eng. J.* **2012**, *184*, 1−8.
(38) Deng, Y. Q.; White, J. C.; Xing, B. S. Interactions between engineered nanomaterials and agricultural crops: implications for food safety. *J. Zhejiang Univ., Sci., A* **2014**, *15* (8), 552−572.
(39) Zhou, D.; Jin, S.; Li, L.; Wang, Y.; Weng, N. Quantifying the adsorption and uptake of CuO nanoparticles by wheat root based on chemical extractions. *J. Environ. Sci.* **2011**, *23* (11), 1852−1857.
(40) Servin, A. D.; Morales, M. I.; Castillo-Michel, H.; Hernandez-Viezcas, J. A.; Munoz, B.; Zhao, L.; Nunez, J. E.; Peralta-Videa, J. R.; Gardea-Torresdey, J. L. Synchrotron Verification of TiO2 Accumulation in Cucumber Fruit: A Possible Pathway of TiO2 Nanoparticle Transfer from Soil into the Food Chain. *Environ. Sci. Technol.* **2013**, *47* (20), 11592−11598.
(41) Gardea-Torresdey, J. L.; Rico, C. M.; White, J. C. Trophic Transfer, Transformation, and Impact of Engineered Nanomaterials in Terrestrial Environments. *Environ. Sci. Technol.* **2014**, *48* (5), 2526−2540.
(42) Zhu, H.; Han, J.; Xiao, J. Q.; Jin, Y. Uptake, translocation, and accumulation of manufactured iron oxide nanoparticles by pumpkin plants. *J. Environ. Monit.* **2008**, *10* (6), 713−717.
(43) Judy, J. D.; Unrine, J. M.; Rao, W.; Wirick, S.; Bertsch, P. M. Bioavailability of Gold Nanomaterials to Plants: Importance of Particle Size and Surface Coating. *Environ. Sci. Technol.* **2012**, *46* (15), 8467−8474.
(44) Sabo-Attwood, T.; Unrine, J. M.; Stone, J. W.; Murphy, C. J.; Ghoshroy, S.; Blom, D.; Bertsch, P. M.; Newman, L. A. Uptake, distribution and toxicity of gold nanoparticles in tobacco (*Nicotiana xanthi*) seedlings. *Nanotoxicology* **2012**, *6* (4), 353−360.
(45) Lee, W. M.; An, Y. J.; Yoon, H.; Kweon, H. S. Toxicity and bioavailability of copper nanoparticles to the terrestrial plants mung bean (*Phaseolus radiatus*) and wheat (*Triticum aestivum*): Plant agar test for water-insoluble nanoparticles. *Environ. Toxicol. Chem.* **2008**, *27* (9), 1915−1921.
(46) Holbrook, D. R.; Motabar, D.; Quiñones, O.; Stanford, B.; Vanderford, B.; Moss, D. Titanium distribution in swimming pool water is dominated by dissolved species. *Environ. Pollut.* **2013**, *181*, 68−74.
(47) Wang, H.; Wick, R. L.; Xing, B. Toxicity of nanoparticulate and bulk ZnO, Al2O3 and TiO2 to the nematode *Caenorhabditis elegans*. *Environ. Pollut.* **2009**, *157* (4), 1171−1177.

DOI: 10.1021/acs.est.7b01364
Environ. Sci. Technol. 2017, 51, 10615−10623

Supporting Information

Multiple method analysis of TiO_2 nanoparticle uptake in rice (*Oryza sativa* L.) plants

Yingqing Deng[a,†], Elijah J. Petersen[b,†,*], Katie E. Challis[c], Savelas A. Rabb[d], R. David Holbrook[e], James F. Ranville[c], Bryant C. Nelson [b], Baoshan Xing[a,*]

[a] Stockbridge School of Agriculture, University of Massachusetts Amherst, Amherst, Massachusetts 01003, United States

[b] Biosystems and Biomaterials Division, National Institute of Standards and Technology, Gaithersburg, Maryland 20899, United States

[c] Department of Chemistry, Colorado School of Mines, Golden, Colorado 80401, United States

[d] Chemical Sciences Division, National Institute of Standards and Technology, Gaithersburg, Maryland 20899, United States

[e] Materials Measurement Science Division, National Institute of Standards and Technology, Gaithersburg, Maryland 20899, United States

[†]**Both authors contributed equally to this work.**

22 pages total including 3 tables and 9 figures.

Supplemental Methods

ICP-OES analysis of plant samples and settling of TiO_2 NPs and BPs

The plant samples were subdivided and classified as shoots and roots and digested using a CEM MARS5 microwave sample preparation system (Matthews, NC). The samples (0.02 g to 0.2 g) were placed in Teflon vessels with 10 mL of concentrated HNO_3 (VERITAS Redistilled, GFS Chemicals, Powell, OH) and 1 mL of concentrated HF (Reagent ACS, GFS Chemicals) and allowed to pre-digest overnight. The microwave digestion program was as follows: power, 1600 W; ramp, 20 min; hold temp, 200 °C; hold time, 15 min. All samples were evaporated to near dryness and reconstituted to contain 1 % HNO_3/1 % HF. The final samples yielded a target Ti mass fraction of 30 µg/kg with 20 µg/kg Sc as an internal standard.

Specimens for the settling experiments were removed from the vials that the samples were shipped in from Amherst, MA to Gaithersburg, MD, placed in polyethylene bottles, acidified with 0.15 mL of HNO_3 and 0.15 mL of HF and heated overnight in an oven at 70 °C to 80 °C to promote dissolution. After cooling, the solutions were diluted to 1 % HNO_3/1 % HF. Preliminary analyses of the control solutions showed the TiO_2 mass fractions were much lower than expected. Further investigations determined that during the storage period, some of the TiO_2 had settled to the bottom of the vials and not been fully removed. To complete the removal of TiO_2 from the vial, 0.2 mL HNO_3 and 0.2 mL HF were added to the vials and allowed to sit in the oven overnight. Afterwards, the solutions were cooled and diluted as appropriate. The final samples yielded a target Ti mass fraction of 75 µg/kg with 20 µg/kg Sc as an internal standard.

Both sets of samples were analyzed by a PerkinElmer 5300DV ICP-OES instrument (Shelton, CT). The sample introduction system of the ICP-OES consisted of a MiraMist nebulizer and cyclonic spray chamber. Operating parameters were optimized for robust conditions (power: 1.5 kW, nebulizer gas: 0.6 L/min and sample uptake: 0.7 mL/min). The calibration was performed by using the method of standard additions to compensate for any matrix effects. Each sample was split into two solutions and one solution was spiked with the analyte. A 0.5 g spike was taken from the Ti spike stock solution and added to a 5 g sample

solution. The Ti spike stock solution was prepared from SRM 3162a Titanium Standard Solution (Lot# 060808). Each sample measurement comprised five replicates, and each solution was measured two different times for the analysis.

spICP-MS analysis of the plant samples

Plants exposed to 50 mg/L of nanoparticle (NP) TiO_2 or 50 mg/L of bulk particle (BP) TiO_2 and unexposed control plants were digested by acid microwave and enzyme methods for subsequent analysis by single particle ICP-MS (spICP-MS). Prior to digestion, plants were flash frozen in liquid nitrogen and pulverized manually using agate mortars and pestles. Individual whole plants were prepared for each of the triplicate measurements of both digestion methods. In some cases, roots and stems, which had previously been separated, were combined to represent a whole plant. Plants were weighed and transferred to a Teflon™ digestion vessel for the microwave acid digestion or to a 15mL polypropylene Falcon™ tube for the enzyme digestion.

Acid digestions were performed using a modification of EPA 3051 and 3052 methods.[1, 2] The heating scheme from method 3052 was applied (ramp to 180 °C ± 5 °C in 5.5 min and hold at this temperature for 9.5 min) [1]. The dual acid digestion (3 mL concentrated HCl and 9 mL concentrated HNO_3) from EPA method 3051 was used with trace metal grade strong acids (Fisher Scientific; Pittsburgh, PA). After the digestion procedure, samples were diluted with ultra-pure 18 MΩ water(Millipore) to 50mL in Falcon™ tubes and stored at room temperature until analysis. Acid digested samples were further diluted with ultra-pure water to a 2 % acid concentration prior to analysis by single particle ICP-MS. A portion of the acid-digested samples (acid digestion control without particles, acid-digested NPs, and acid-digested BPs) and untreated NPs and BPs were syringe filtered through an alumina based inorganic membrane filter (Anotop 25 by Whatman®, 0.02 µM pore size and 25 mm diameter) and analyzed by ICP-OES to determine if dissolved titanium was present; the detection limit was 0.0006 mg/L Ti at emission wavelength of 334.940 λ. No results were greater than the detection limit for any of the samples. A high solids Meinhard Nebulizer

was used with a cyclonic spray chamber. Nebulizer gas flow rate of 0.65 L/min and sample uptake rate of 1.2 mL/min were used. Plasma conditions were robust with a 16 mL/min Ar flow and power of 1.5 kW.

Enzyme digestion was performed using Macerozyme R-10 purchased from bioWorld (Dublin, OH). Enzyme solutions were prepared in 1.3 mmol/L citrate-phosphate (Citric Acid Monohydrate: Fisher Scientific; Pittsburgh, PA; Sodium Phosphate Dibasic: Sigma Aldrich; St. Louis, MO) buffer prepared at pH 4.0 by adding 1 g of enzyme to 100 mL of buffer.[3] Each pulverized plant was digested in 5 mL of enzyme solution. Digestions were carried out in a dry bath (Genemate Digital Dry Bath, Bioexpress) held at 37° C while mixing on an orbital shaker (Rotomix Type 50800, Thermolyne) for 48 h with samples taken at 24 h and 48 h time points. Samples were diluted 100 x prior to analysis by spICP-MS. For some samples, additional dilution was required for proper analysis by spICP-MS.

Controls included NP and BP TiO_2 suspended in ultrapure water using the same probe and sonication approach described in the methods section. Both particles were carried through the acid and enzyme digestion procedures. Controls of blank samples (deionized water without particles) were treated with the microwaved acid or enzyme digestion method. These samples and a solution of the enzymes without undergoing the treatment process were also analyzed by spICP-MS.

All single particle analyses were performed on a quadrupole ICP-MS (NexION 300D series, Perkin Elmer). Data was collected using the Nano Application Module in Perkin Elmer's Syngistix™ for ICP-MS software. Following comparison of Ti 48.9 and Ti 47.9, titanium was measured using the most abundant isotope of 47.948 amu due to better nanoparticle size detection and no evidence of ^{48}Ca interference. A single particle fast scan method[4] utilizing a 100 µs dwell time for 60 s was applied to all measurement in standard ICP-MS operation mode. Instrument transport efficiency was determined by the mass based method prior to each analysis.[5] A NIST 60 nm gold nanoparticle standard (RM 8013) was used for the transport efficiency calibration (SPEX CertiPrep®; Metuchen, NJ) [1]. A low flow glass nebulizer from Meinhard (Golden, CO) was used along with a Perkin Elmer cyclonic spray chamber. Nebulizer gas flow was 0.88 L/min to 0.98

L/ min depending on daily optimization. Sample introduction rate was 0.3 mL/min. Plasma gas was 16L/ min with a 1600W RF power. QID was tuned daily.

Data was analyzed by determining the background +3σ for the blank and removing all points less than or equal to the value.[5] In the fast scan analysis, two consecutive data points above the 3σ values were necessary to consider the peak a particle detection. A peak's total counts were determined by summing all the consecutive counts above background+3σ. Data was processed for background filtering, peak summing, and size determination using Microsoft Excel. Although more advanced methods of signal detection have been developed,[6] at the time of this analysis the software for the signal deconvolution method had not yet been published with the ability to analyze fast scan data. The peaks were converted to nanoparticle size assuming a spherical shape and TiO_2 density of 4.23 g/cm^3. Graphs were made using Origin Pro Student Version Software.

Determination of CAT, POD, APX and SOD activities

To determine the activities of antioxidant enzymes, fresh plant tissues were frozen with liquid nitrogen and ground before extraction. Enzyme activity units (U) were expressed relative to total protein content (U/mg protein). The total soluble protein content of enzyme extracts was determined using a Bradford assay.[7] To examine if the presence of BPs could bias the assay results, TiO_2 NPs and BPs were added directly into the extract from control plants and the enzyme activities using the method described in the following paragraph were determined and compared to samples without added particles. The TiO_2 concentrations added corresponded to the highest Ti concentration measured in plant samples (2000 µg/g) during the elemental analyses. The results did not show a significant difference between samples with or without the added particles.

Determination of CAT was modified from the method by Gallego et al..[8] Homogenized tissues were extracted with 50 mmol/L phosphate buffer solution (pH 7.0), vortexed for 1 min and then centrifuged for 20 min at 3500 ×g and 4 °C (Eppendorf 5804). A mixture of 200 µL supernatant and 1800 µL 10 mmol/L

H_2O_2 were analyzed on a Genesys-10 UV/Vis spectrophotometer (Thermo Spectronic, Rochester, USA) at 240 nm for 3 min. The activities were calculated from the first linear section of slope between 0.5 min and 2 min. Peroxidase POD was extracted following the same method on CAT and enzyme extract was reacted with 0.1 mL 4 % guaiacol. The increase in absorbance was monitored at 470 nm for 2 min and one unit of enzymatic activity represented 0.01 absorbance change/min. The method of APX determination was modified from Chen et al..[9] Homogenized tissues were extracted with phosphate buffer (pH 7.0) containing 0.1 mmol/L EDTA, 0.1 mmol/L ascorbate, and 2 % (v/v) ß-mercaptoethanol. The oxidation rate of ascorbic acid was determined in a reaction buffer composed of 50 mmol/L phosphate buffer (pH 7.0) and 25 mmol/L ascorbic acid. The reaction was initiated by addition of 10 µL 10 % (v/v) H_2O_2. APX activity, which was reflected by the oxidation rate of ascorbic acid, was determined by following the decrease in absorbance at 290 nm for 5 min. SOD activity was assayed using the photochemical nitro blue tetrazolium (NBT) method. 0.5 g grounded tissues was extracted with 5 mL extraction butter consisting of 50 mmol/L phosphate (pH 7.8), 0.1 % (w/v) BSA, 0.1% (w/v) ascorbate, and 0.05 % (w/v) ß-mercaptoethanol. Supernatant sample was reacted with 50 mmol/L phosphate buffer (pH 7.8), 9.9 mmol/L L-methionine, 57 µM NBT, 0.025% (v/v) Triton X-100 and 0.0044% (w/v) riboflavin. The photoreduction of NBT was measured at 560 nm and an inhibition curve was made against different volumes of extract. One unit of SOD was determined as that being present in the volume of extract that caused inhibition of the photo-reduction of NBT by 50 %.

DNA damage measurements

In order to determine the amount of particle-induced DNA damage, the levels of three oxidatively modified DNA bases [8-hydroxyguanine (8-OH-Gua), 5-hydroxy-5-methylhydantoin (5-OH-5MeHyd) and hydroxyadenine (8-OH-Ade)] were measured in rice plants after exposure to the TiO_2 NPs or BPs for 24 h. Genomic plant DNA was extracted from the rice plants using a modified cetyltrimethylammonium bromide (CTAB) extraction buffer method.[10] Before instrument analysis, DNA aliquots of 50 µg were spiked with stable isotopically-labeled analogs of each base lesion (8-OH-Gua-$^{15}N_5$, 5-OH-5-MeHyd-^{13}C,$^{15}N_2$ and 8-

OH-Ade-$^{13}C,^{15}N_2$). The determination of DNA lesions was performed on a GC/MS system (6890N Network GC coupled to a 5973 Network Mass Selective Detector, Agilent Technologies, Inc., Rockville, MD) using previously described methodology.[11]

Supplemental Results and Discussion

Characterization of TiO_2 particles

The TiO_2 NPs and BPs were imaged and analyzed using TEM (Figure S1) and ImageJ, respectively. The NPs had a primary size of approximately 27.5 nm ± 2.7 nm (n=300; uncertainty indicates standard deviation), while 95 % of the primary particle size of the BPs were between 65 nm and 232 nm; however, the substantial number of large agglomerates made it challenging to precisely determine the primary particle size of the BPs. The result for the NPs was in good agreement with the reported ranges (19 nm to 37 nm) in the manufacturer's specifications, and similar to the previously published value of 24 nm.[12] ICP-OES results of the initial NP and BP suspensions indicated lower concentrations for the NP suspensions than expected: 3 mg/L and ≈ 40 mg/L, for the nominal concentration 5 mg/L and 50 mg/L conditions, respectively, while the concentrations for the BPs were close to the nominal values (Table S1). The cause of the lower values for the NPs but not the BPs was unclear as incomplete digestion and ionization should affect BP to a greater degree than NPs. Because plant exposure to NPs or BPs lasted for 24 h, the hydrodynamic diameter of TiO_2 NPs suspended in Milli-Q water was determined using DLS for samples before and after exposure with plants or in the test containers after 24 h without plants. Measurements performed after 24 h utilized liquid from near the top of the exposure container without further sonication. In NP suspensions without plants, the hydrodynamic diameters of TiO_2 NPs remained relatively unchanged over time for both concentrations (Table S2). In contrast, the NP suspensions in the presence of plants showed agglomeration and sedimentation with white agglomerates visible on the plant roots. The hydrodynamic diameter of TiO_2 NPs increased several fold in the presence of plants: from 177 nm ± 1 nm to 363 nm ± 24 nm and from 184 nm ± 2 nm to 363 nm ± 24 nm and 884 nm ± 155 nm in the 5 mg/L and 50 mg/L suspensions, respectively. In agreement with these results, ≈ 90 % of the NPs for the 50 mg/L condition settled during the 24 h period while ≈ 33 % settled for the 5 mg/L condition (Table S1). These results indicated strong agglomeration occurred in the presence of plants. It was previously reported that rice roots could release a complex mixture of highly soluble carbohydrates (e.g., glucose, mannose,

galactose), organic acids (e.g., citric, tartaric, succinic) and amino acids (e.g., proline, valine, alanine, glycine).[13-15] It is possible that these organic exudates were adsorbed onto the particle surfaces through metal-binding functional groups, although this was not tested in this study. As such, the exudates could alter electrostatic repulsion and steric repulsion between particles and accelerate agglomeration in NP suspensions.[16-18] These interactions between TiO_2 NPs and root exudates are prevalent in natural settings, and would likely affect the biocompatibility, uptake, and bioaccumulation of NPs in plants. TiO_2 BPs were not included in this discussion due to fast deposition, limited suspended particle numbers and agglomerates that were greater than the DLS measurement range (the upper size limit indicated by the manufacturer is 3 μm but results in our previous analysis indicated that it was challenging to achieve reproducible results with particles > 1 μm). Substantial settling was also shown in the ICP-OES results, which indicated that > 75 % of the BPs settled for the 5 mg/L and 50 mg/L conditions (Table S1). These results are unsurprising given that larger particles typically agglomerate more quickly than smaller ones of the same composition.[19, 20] However, additional research is needed in order to study the fate of TiO_2 NPs in natural soil environments.

Antioxidant enzymes and oxidatively induced DNA base damage

Rice plants may be affected physiologically from the uptake and accumulation of the NPs and BPs as the plant cells attempt to maintain cellular homeostasis. Therefore, four typical housekeeping antioxidant enzymes (SOD, APX, CAT and POD) were measured immediately after particle exposure and then again after being returned to Hoagland's media for 3 d in order to assess possible impact of TiO_2 exposure on the plant (Figures S7 and S8). While the plants tested 3 d after particle exposure did not show statistically significant changes ($p > 0.05$) to any enzyme (Figure S8), the activities of two major H_2O_2-detoxifying enzymes, CAT and APX, were significantly elevated when the plants were treated with the higher concentration of TiO_2 regardless of the particle size for the samples extracted immediately after particle exposure (Figure S7). Interestingly, NP-treated plants tend to utilize more APX enzymes while BP-treated plants were more dependent on CAT for redox regulation. Given that APX enzymes are localized in several subcellular compartments whereas CAT is mostly localized in the peroxisome,[21] it is possible that the NPs

were more distributed in the cytoplasm and triggered H_2O_2 over-production in various subcellular compartments. Immediately after TiO_2 NP or BP exposure during the first week, GC/MS analyses on the DNA extracted from the rice plantlets did not show a statistically significant accumulation of oxidatively-induced DNA base lesions in comparison to the measured lesion levels in an unexposed control sample (Figure S9). This finding indicates that the antioxidant enzymes were sufficient to avoid detectable oxidative damage to the DNA bases.

Supplemental Tables

Table S1. Initial concentrations of NPs and BPs after settling for 24 h in the presence and absence of plants. Values indicate mean values of triplicate measurements and uncertainties indicate standard deviation values.

	stock suspension (mg/L)	DI H_2O without plants (mg/L)	DI H_2O with plants (mg/L)
NP 5 mg/L	3.02 ± 0.13	3.42 ± 0.54	1.97 ± 0.35
NP 50 mg/L	39.68 ± 1.11	39.89 ± 1.13	3.75 ± 1.51
BP 5 mg/L	5.60 ± 0.30	1.79 ± 0.19	1.39 ± 0.17
BP 50 mg/L	50.51 ± 0.54	4.35 ± 0.70	6.20 ± 2.84

Table S2. Hydrodynamic diameter (size) of TiO_2 nanoparticles in Milli-Q water before and after plant exposure. Values indicate mean values of triplicate measurements and uncertainties indicate standard deviation values.

	Before exposure		After exposure, without plants		After exposure, with plants	
	Hydrodynamic diameter (nm)	Polydispersity index	Hydrodynamic diameter (nm)	Polydispersity index	Hydrodynamic diameter (nm)	Polydispersity index
TiO_2 NP 5 mg/L	177 ± 2	0.193 ± 0.009	199 ± 14	0.143 ± 0.027	363 ± 24	0.276 ± 0.011
TiO_2 NP 50 mg/L	184 ± 2	0.182 ± 0.002	151 ± 6	0.149 ± 0.026	884 ± 155	0.651 ± 0.064

All measurements represent mean ± SD; N = 3

Table S3: Average number of nanoparticles detected per gram of plant tissue for control, NP-exposed and BP-exposed plants. Values were calculated from number of particles detected during analysis and indicate mean ±standard deviation values (n=3).

	Particle number/g plant tissue		
Samples	Acid	24 h Enzyme	48 h Enzyme
Control Plants	$1.4 \times 10^9 \pm 1.3 \times 10^7$	$1.5 \times 10^9 \pm 6.4 \times 10^8$	$2.3 \times 10^9 \pm 1.8 \times 10^9$
NP Plants	$7.1 \times 10^{10} \pm 2.7 \times 10^8$	$4.0 \times 10^{10} \pm 2.4 \times 10^{10}$	$4.4 \times 10^{10} \pm 2.2 \times 10^{10}$
BP Plants	$6.3 \times 10^9 \pm 1.3 \times 10^7$	$7.1 \times 10^8 \pm 1.1 \times 10^8$	$6.8 \times 10^8 \pm 4.7 \times 10^7$

Supplemental Figures

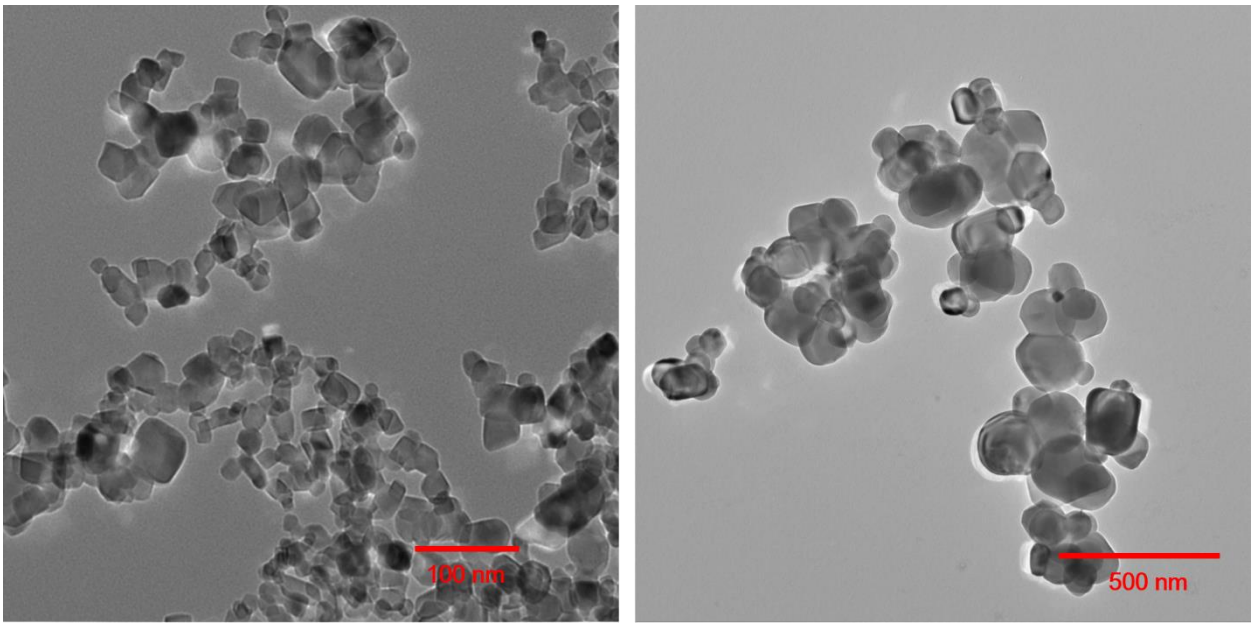

Figure S1. TEM images of TiO_2 NPs (left) and BPs (right).

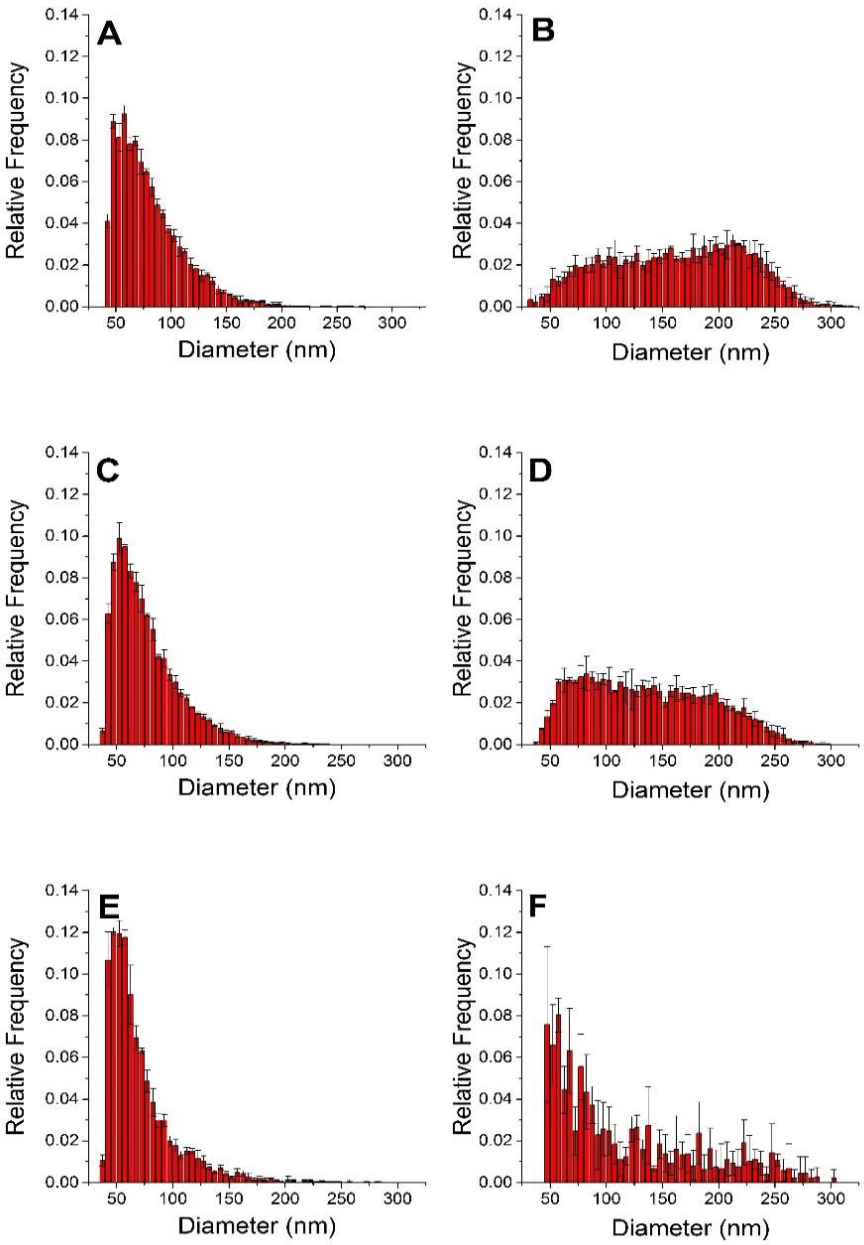

Figure S2. spICP-MS analysis of 48 h enzymatic digestion data for NPs and BPs. Size distributions are normalized to relative frequency. All graphs are the averages of triplicate samples and error bars represent standard deviation values. Untreated NPs (A) and BPs (B) in water. NPs (C) or BPs (D) after 48 h enzymatic digestion. Plants exposed to NPs (E) or BPs (F) and then enzyme digested for 48 h.

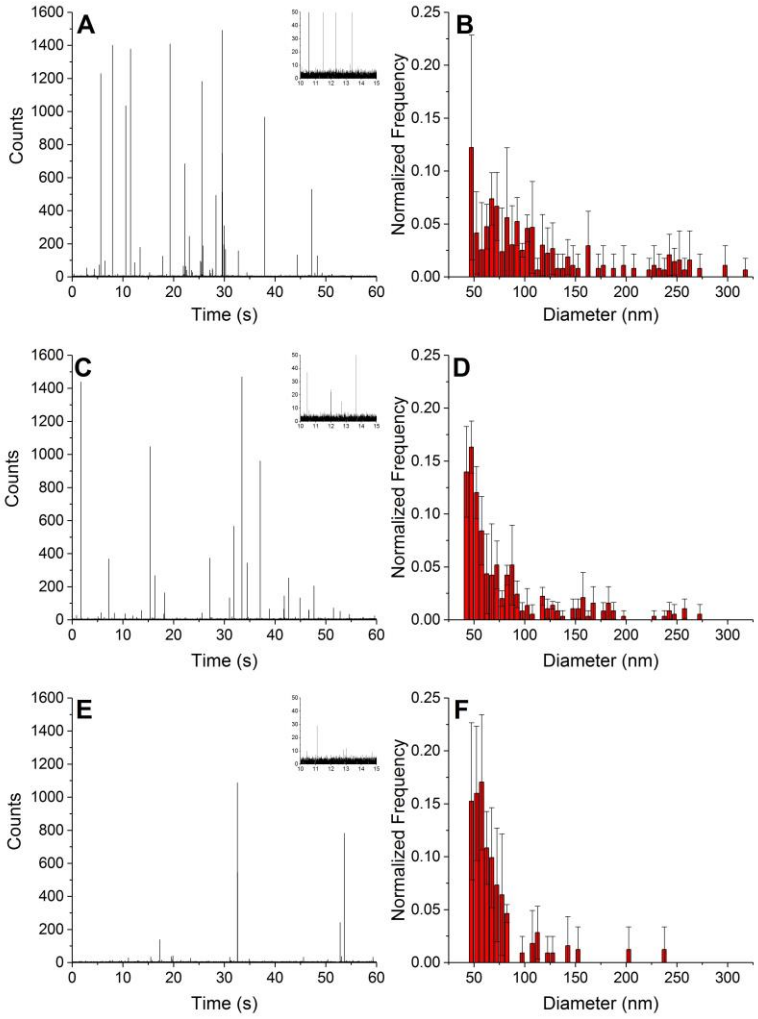

Figure S3: spICP-MS analysis of reagent control samples (without particles) treated with the different digestion procedures. Example graphs of raw single particle data, pulses are interpreted as particles, for the acid treatment (A) or the enzymatic 24 h (C) or 48 h treatment (E) samples; one graph from one of the triplicate measurements is shown. Insets zoom in on five seconds of data to reveal the background. Relative frequency graphs of control samples for the acid treatment (B) or the enzymatic 24 h (D) or 48 h. treatments (F); graphs are the averages of triplicate samples and error bars represent standard deviation values

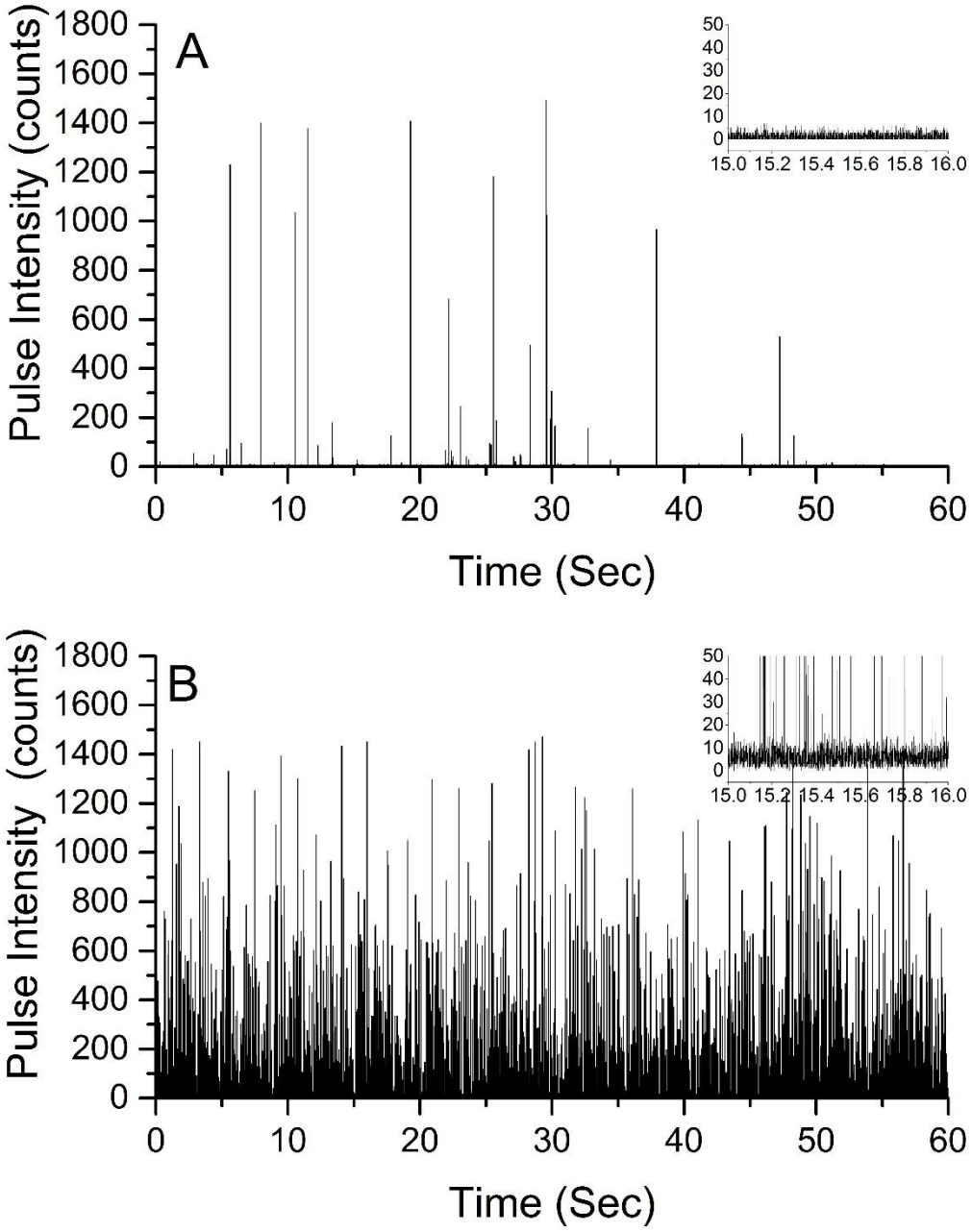

Figure S4: Example of spICPMS signals detected in (A) acid matrix and (B) an acid-digested NP-exposed plant. Insets zoom in on one second of data; only pulses with intensities higher than 16 counts were considered particles.

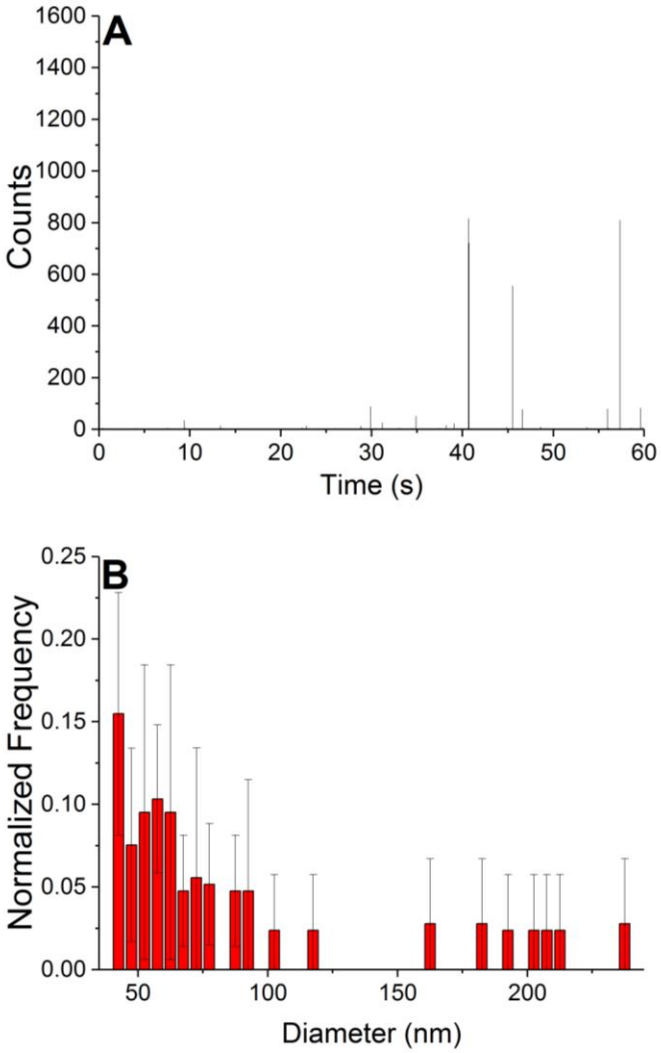

Fig S5: Raw data for MilliQ water (A). Relative frequency from three samples of MilliQ (B). Note that the number of peaks above the background for each MilliQ sample was less than 15 for an analysis of a similar volume as for the other samples. Data shown in part B are the averages of triplicate samples and error bars represent standard deviation values.

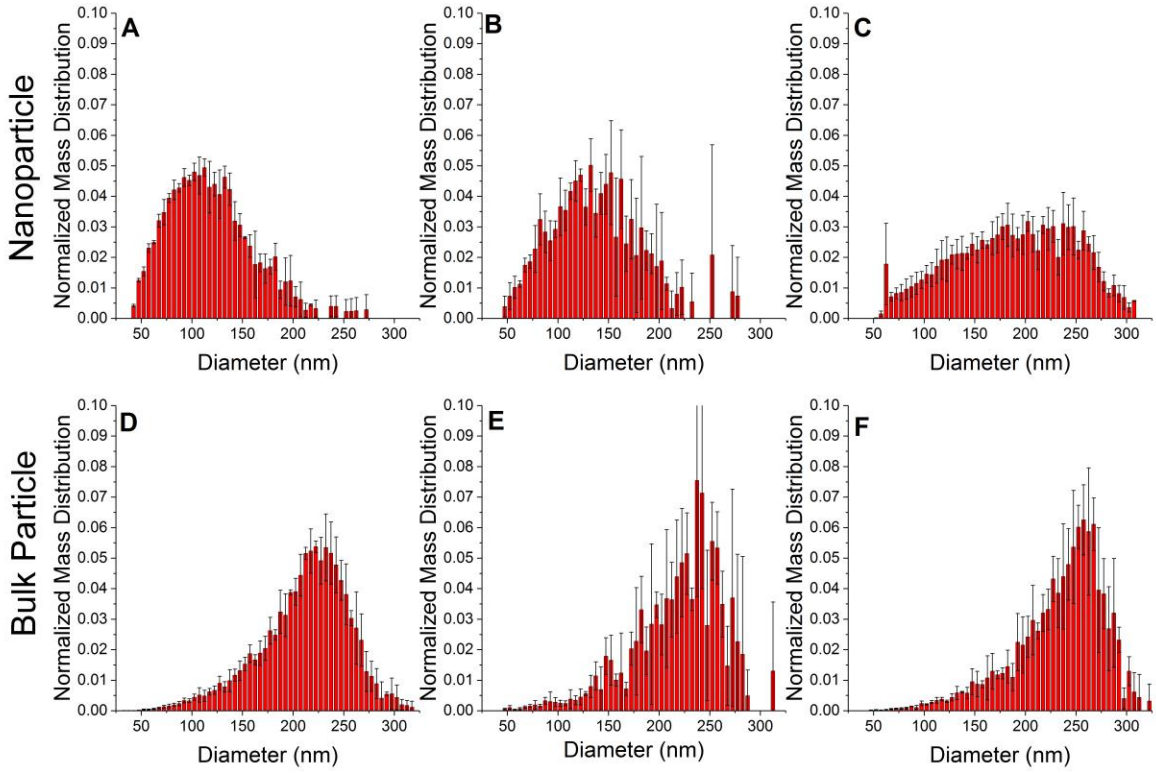

Figure S6: Mass weighted size distribution summary of spICP-MS results for the acid digestion procedure samples. Results from control (not treated) NPs (A) and BPs (D). NP (B) and BP (E) samples treated using the acid digestion procedure. Plant samples exposed to NPs (C) or BPs (F) treated with the acid digestion procedure. Graphs are the averages of triplicate samples and error bars represent standard deviation values.

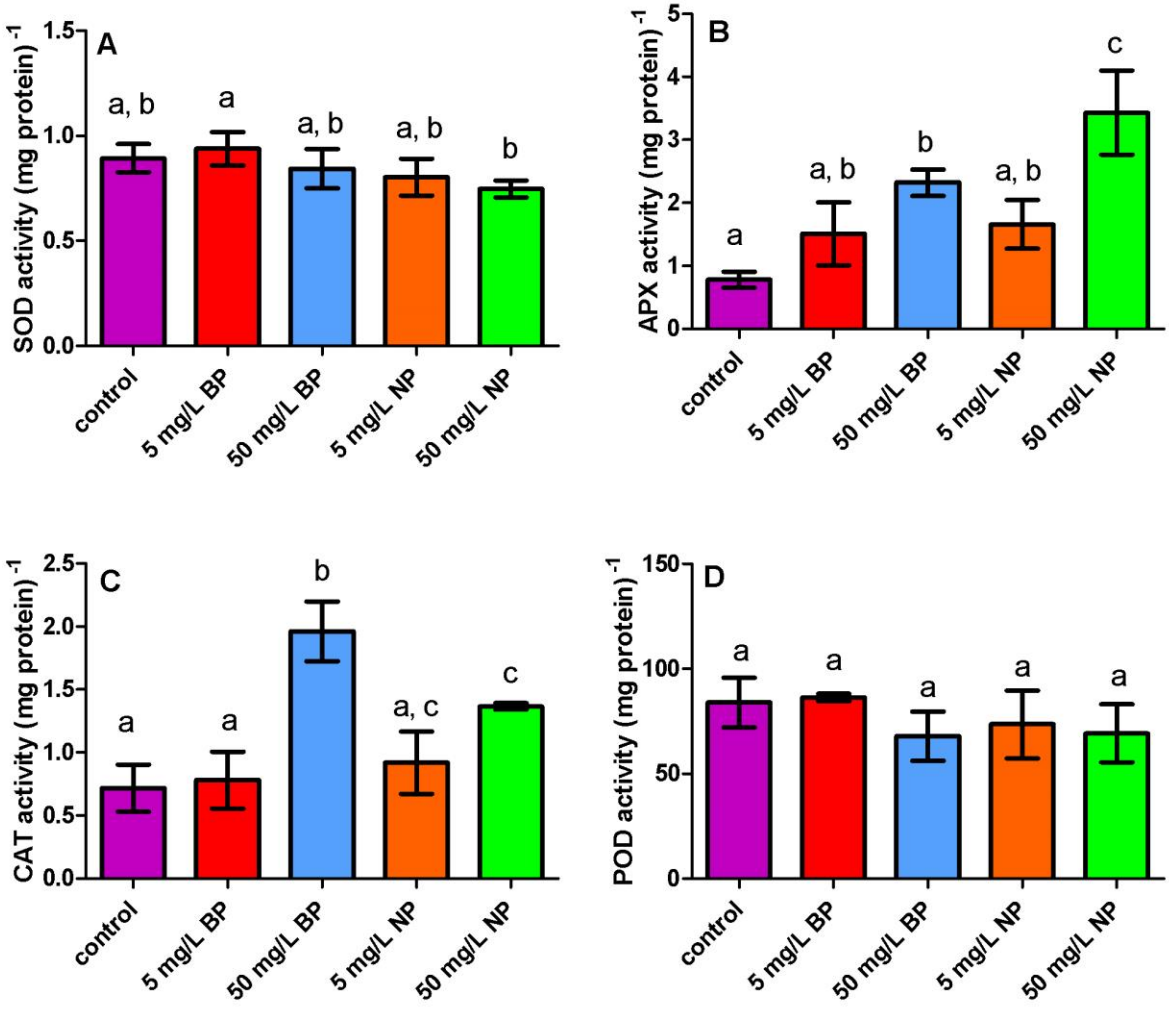

Figure S7. Content of (a) superoxide dismutase (SOD), (b) ascorbate peroxidase (APX), (c) catalase, (CAT) and (d) peroxidase (APX) in *O. sativa* whole plant extracts. Extraction of enzymes was performed immediately after exposure to TiO_2 NP and BP suspensions for 24 h while control plants were exposed to distilled water for during this period. Each bar represents the mean ± SD of at least three replicates. Data were analyzed using one-way Analysis of Variance (ANOVA) followed by Tukey's multiple comparison test. Bars with the same letter are not significantly different.

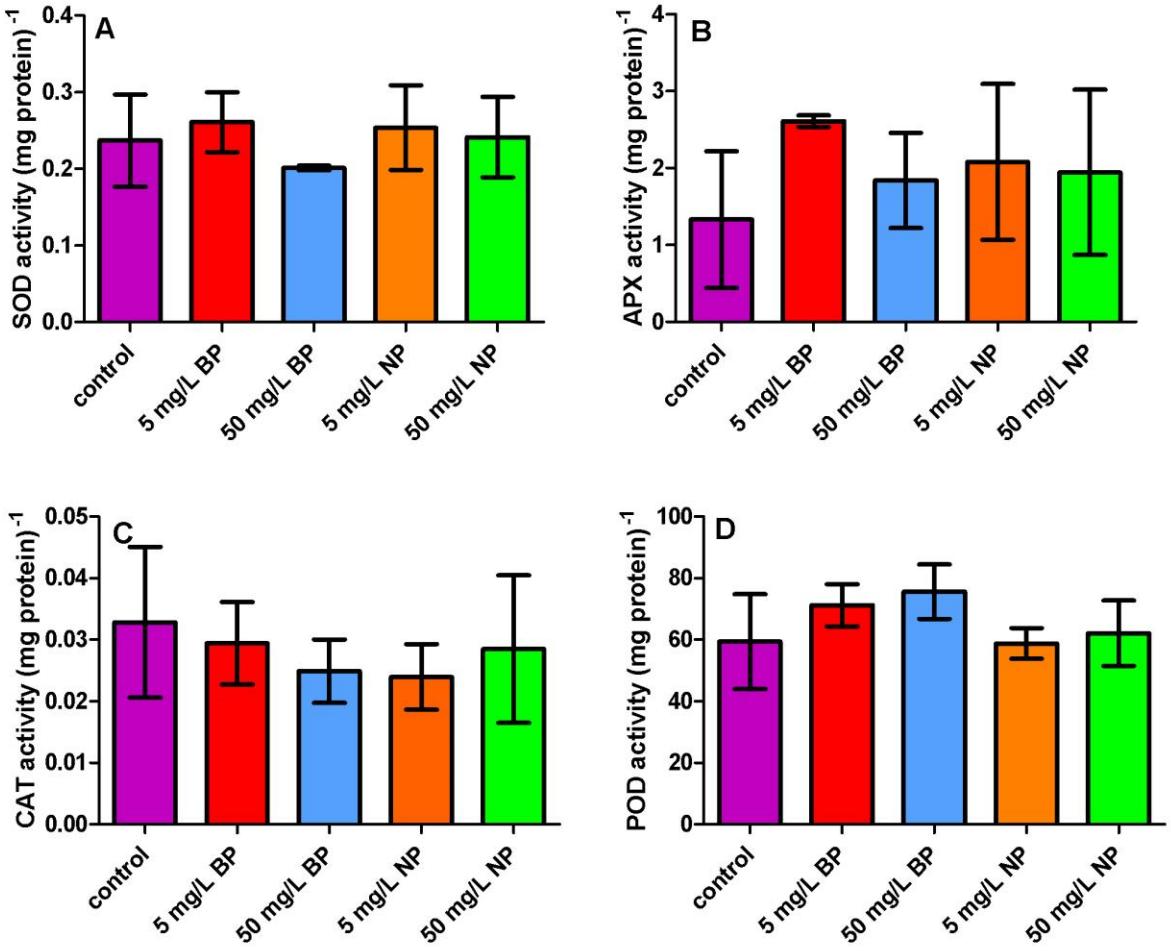

Figure S8. Content of (a) superoxide dismutase (SOD), (b) ascorbate peroxidase (APX), (c) catalase, (CAT) and (d) peroxidase (APX) in *O. sativa* whole plant extracts. Extraction of enzymes was performed 3 d after the plants had been exposed to particles. Data were analyzed using using one-way Analysis of Variance (ANOVA) followed by Tukey's multiple comparison test. No statistically significant differences were observed for any of the enzymes. Each bar represents the mean ± SD of at least three replicates.

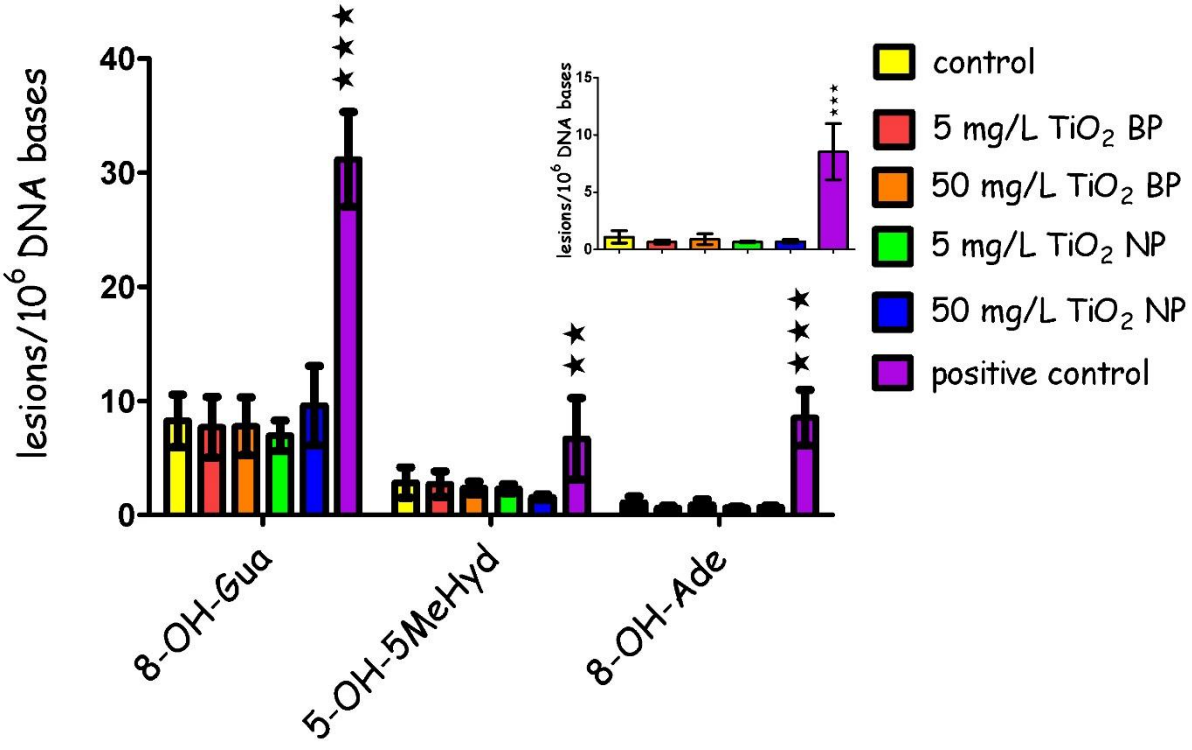

Figure S9. Oxidatively-induced DNA base lesions (8-OH-Gua, 5-OH-5MeHyd, and 8-OH-Ade) did not accumulate after in rice plants exposed to either 5 mg/L or 50 mg/L TiO2 NPs and BPs. All data points represent the mean of 4 or 5 independent measurements. Error bars represent standard deviations. The negative control was an unexposed rice plant and the positive control was calf-thymus DNA. Asterisks indicate statistically significant results compared to the negative control samples using one-way Analysis of Variance (ANOVA) followed by Dunnett's multiple comparison test. Two and three asterisks indicate $p < 0.01$ and 0.001, respectively.

References

1. Agency of Environmental Protection, Method 3052 Microwave Assisted Acid Digestion of Siliceous and Organincally Based Matrices. **1996**.
2. Agency of Environmental Protection, Method 3051a: Microwave Assisted Digestion of Sediments, Sludges, Soils, and Oils Revision 1. **2007**.
3. Dan, Y.; Zhang, W.; Xue, R.; Ma, X.; Stephan, C.; Shi, H., Characterization of Gold Nanoparticle Uptake by Tomato Plants Using Enzymatic Extraction Followed by Single-Particle Inductively Coupled Plasma–Mass Spectrometry Analysis. *Environ Sci & Tech* **2015,** *49*, (5), 3007-3014.
4. Montano, M. D.; Badiei, H. R.; Bazargan, S.; Ranville, J. F., Improvements in the detection and characterization of engineered nanoparticles using spICP-MS with microsecond dwell times. *Environ Sci Nano* **2014,** *1*, (4), 338-346.
5. Pace, H. E.; Rogers, N. J.; Jarolimek, C.; Coleman, V. A.; Higgins, C. P.; Ranville, J. F., Determining Transport Efficiency for the Purpose of Counting and Sizing Nanoparticles via Single Particle Inductively Coupled Plasma Mass Spectrometry. *Anal. Chem.* **2011,** *83*, (24), 9361-9369.
6. Cornelis, G.; Hassellov, M., A signal deconvolution method to discriminate smaller nanoparticles in single particle ICP-MS. *J Anal At Spectrom* **2014,** *29*, (1), 134-144.
7. Zor, T.; Seliger, Z., Linearization of the bradford protein assay increases its sensitivity: Theoretical and experimental studies. *Anal. Biochem.* **1996,** *236*, (2), 302-308.
8. Gallego, S. M.; Benavides, M. P.; Tomaro, M. L., Effect of heavy metal ion excess on sunflower leaves: Evidence for involvement of oxidative stress. *Plant Sci.* **1996,** *121*, (2), 151-159.
9. Chen, G. X.; Asada, K., Ascorbate peroxidase in tea leaves: Occurrence of 2 isozymes and the differences in their enzymatic and molecular properties. *Plant Cell Physiol* **1989,** *30*, (7), 987-998.
10. Michiels, A.; Van den Ende, W.; Tucker, M.; Van Riet, L.; Van Laere, A., Extraction of high-quality genomic DNA from latex-containing plants. *Anal. Biochem.* **2003,** *315*, (1), 85-89.
11. Atha, D. H.; Wang, H. H.; Petersen, E. J.; Cleveland, D.; Holbrook, R. D.; Jaruga, P.; Dizdaroglu, M.; Xing, B. S.; Nelson, B. C., Copper Oxide Nanoparticle Mediated DNA Damage in Terrestrial Plant Models. *Environ Sci & Tech* **2012,** *46*, (3), 1819-1827.
12. Taurozzi, J. S.; Hackley, V. A.; Wiesner, M. R., A standardised approach for the dispersion of titanium dioxide nanoparticles in biological media. *Nanotoxicology* **2012**.
13. Bacilio-Jiménez, M.; Aguilar-Flores, S.; Ventura-Zapata, E.; Pérez-Campos, E.; Bouquelet, S.; Zenteno, E., Chemical characterization of root exudates from rice (Oryza sativa) and their effects on the chemotactic response of endophytic bacteria. *Plant Soil* **2003,** *249*, (2), 271-277.
14. Aulakh, M. S.; Wassmann, R.; Bueno, C.; Kreuzwieser, J.; Rennenberg, H., Characterization of Root Exudates at Different Growth Stages of Ten Rice (Oryza sativa L.) Cultivars. *Plant Biol* **2001,** *3*, (2), 139-148.
15. Seal, A.; Pratley, J.; Haig, T.; An, M., Identification and Quantitation of Compounds in a Series of Allelopathic and Non-Allelopathic Rice Root Exudates. *J Chem Ecol* **2004,** *30*, (8), 1647-1662.
16. Aiken, G. R.; Hsu-Kim, H.; Ryan, J. N., Influence of Dissolved Organic Matter on the Environmental Fate of Metals, Nanoparticles, and Colloids. *Environ Sci & Tech* **2011,** *45*, (8), 3196-3201.
17. Zhang, Y.; Chen, Y.; Westerhoff, P.; Crittenden, J., Impact of natural organic matter and divalent cations on the stability of aqueous nanoparticles. *Water Res.* **2009,** *43*, (17), 4249-4257.
18. Thio, B. J. R.; Zhou, D.; Keller, A. A., Influence of natural organic matter on the aggregation and deposition of titanium dioxide nanoparticles. *J Hazard Mater* **2011,** *189*, (1–2), 556-563.
19. Su, Y.; Yang, G.; Lu, K.; Petersen, E. J.; Mao, L., Colloidal properties and stability of aqueous suspensions of few-layer graphene: Importance of graphene concentration. *Environ. Pollut.* **2017,** *220, Part A*, 469-477.

20. Elimelech, M.; Gregory, J.; Jia, X.; Williams, R. A., Butterworth-Heinemann: Woburn, 1995; p 68-109
21. Sharma, S. S.; Dietz, K.-J., The relationship between metal toxicity and cellular redox imbalance. *Trends Plant Sci* **2009,** *14*, (1), 43-50.